Crossing of the Equator by the Deep Western Boundary Current in the Western Atlantic Ocean*

M. S. MCCARTNEY

Woods Hole Oceanographic Institution, Woods Hole, Massachusetts

(Manuscript received 31 March 1992, in final form 9 February 1993)

ABSTRACT

Property distributions and geostrophic shear from a hydrographic section near 37°W in the Atlantic Ocean show the deep western boundary current (DWBC) in the North Atlantic Deep Water (NADW) established against the western boundary of the Brazil Basin immediately south of the equator (between 2° and 5°S). The DWBC thus has directly crossed the equator to the South Atlantic following the east-southeast trend of the continental slope isobaths. The estimated DWBC transport of NADW is 35×10^6 m^3 s^{-1}, similar to other estimates from the tropics discussed here. These large DWBC transports are opposed by flow of deep water to the North Atlantic immediately offshore of the DWBC, with as much as two-thirds of the DWBC transport being returned as these recirculations. One recirculation center is the Guiana Basin north of the equator but extends at least a few hundred kilometers south of the equator; another is visible at 11°S in the Brazil Basin. The degree of connection of these two observed recirculations is not established. These recirculations spread the northern source influences over the width of the recirculation (rather than the DWBC width) and efficiently dilute the northern source concentration with South Atlantic influences, with the self-mixing of the recirculation complicating the interpretation of tracer distributions. A further complication occurs for the uppermost levels of the NADW, for the DWBC flows to the Southern Hemisphere beneath an opposing western boundary current of Antarctic Intermediate Water (AAIW), and downgradient property fluxes mutually erode the upper NADW and the AAIW core characteristics. This causes a displacement of the axis of maximum northern source concentration offshore from the axis of maximum transport of upper NADW in the DWBC, a demonstration that the relationship between a tracer tongue and the flow field can be obscure.

1. Introduction

The equatorial Atlantic does not have a great wealth of measurements to describe and quantify its abyssal circulation. McCartney and Curry (1993) quantify the northward transequatorial transport of Antarctic Bottom Water (AABW) using a hydrographic section near 37°W and relate that transport to the AABW transport in the Brazil and Guiana basins, respectively, south and north of the equator. The goal in the present paper is to draw attention to another aspect of that dataset, one involving the manner by which the southward transequatorial flow of North Atlantic Deep Water (NADW) by the deep western boundary current (DWBC) occurs and the intensity of that flow. The DWBC flow across the equator is of fundamental interest because it is a major component of the export of cold water from the North Atlantic to the rest of the World Ocean, with that export being a dominant abyssal circulation feature and one whose description and quantification would be a boon to climate modeling. The net export of cold water is typically estimated as order 15×10^6 m^3 s^{-1}, and is achieved as the difference between a net southward flow of NADW and a net northward flow of AABW (estimated as 4×10^6 m^3 s^{-1} by McCartney and Curry).

The low-latitude circulation of NADW is often conceptualized as a DWBC filament crossing the equator from north to south, with the DWBC dominating the basin transport field at low latitudes. Distributions of NADW properties have been interpreted as indicative of a more complex tropical circulation, with the southward flow of the DWBC bifurcating at the equator into an eastward flow along the equator and a continued southward flow along the western boundary. In the present study the crossing of the equator by the DWBC and related circulations in the Brazil and Guiana basins are examined using an array of hydrographic sections collected over the past decade, Fig. 1. The primary result of this interpretative study is visualized in Fig. 2, two circulation schematics representing two extremes of the possible range of tropical deep circulations. The common denominators of the two extremes are the direct crossing of the equator by DWBC flow along the

* Contribution Number 8039 from the Woods Hole Oceanographic Institution.

Corresponding author address: Dr. Michael S. McCartney, Department of Physical Oceanography, Woods Hole Oceanographic Institution, Woods Hole, MA 02543.

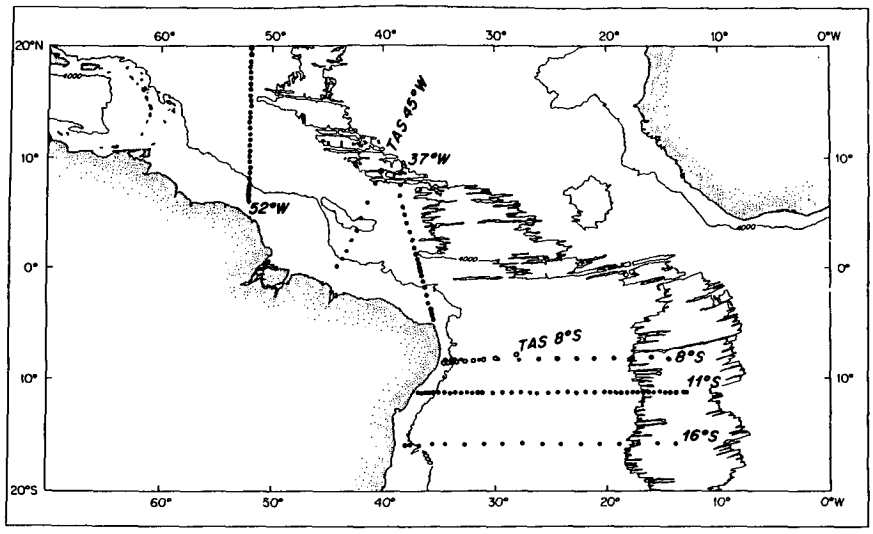

FIG. 1. Chart of the topography of the low-latitude Atlantic and the location of the various stations and sections used in the present study.

western boundary, the presence of recirculating gyre flows in the Brazil and Guiana basins, and the extension of the Guiana abyssal gyre southward of the equator so that there is both northward and southward trans-equatorial flow of NADW near the western boundary. The two extremes represent the uncertainty as to the degree of circulation connection between the recirculations in the northern Brazil Basin between 5° and 10°S.

This paper is structured as follows. Section 2 is a review of aspects of the abyssal circulation of the western tropical Atlantic Ocean drawing on the literature of the past decade. Section 3 documents the crossing of the equator by the DWBC and gives estimates of its transport immediately south of the equator (near 3°S). Section 4 describes evidence for a flow of NADW from the Brazil Basin to the Guiana Basin offshore of the DWBC and relates it to the southern closure of a recirculating gyre in the Guiana Basin. Section 5 discusses the impact on the uppermost part of the DWBC of the counterflowing Antarctic Intermediate Water (AAIW) that lies immediately above it along the western boundary. The impact causes the distribution of the uppermost part of the NADW to be rather different from that of the bulk of the NADW layer. Section 6 documents the existence of a narrow (subbasin scale) and intense recirculating abyssal gyre along the western boundary of the Brazil Basin, and gives estimates of its transport. An attempt to merge these various observations leads to the alternative schematic circulations of Fig. 2. Section 7 gives some summary remarks.

2. Background

The influence of dense water from northern North Atlantic sources on the South Atlantic has been realized since the earliest deep hydrographic measurements, being made particularly apparent by the data collected during the *Meteor* expedition of the 1920s, reported on by Wüst [1935; see also the review by Warren (1981)]. The Stommel and Arons (1960) theory of the abyssal circulation provides a framework for interpreting such observed property distributions and currents. In this framework upwelling of cold water into the base of the thermocline drives, via the planetary vorticity constraint, poleward flow in the interior of ocean basins. Since the cold water sources are at high latitudes and the interior circulation is poleward, often the only route in a basin for conveying the cold water to middle and low latitudes is the DWBC. With the interior flow field completely defined by the basin geometry and the upwelling rate, the DWBC transport at a given latitude in the basin follows from mass balance considerations, given a specification of the location(s) of cold water source(s) of the necessary strength(s). For a basin spanning the equator, there is no interior flow across the equator, and the DWBC flow direction across the equator and its transport follow from the integrated upwelling north and south of the equator and the split of the total required source strength between northern and southern sources.

In his review of the global deep circulation, Warren (1981) noted that one of the inadequacies of the North Atlantic database was the lack of sections across the western boundary between 23°N and the equator suitable for geostrophically estimating the DWBC transport towards the South Atlantic. This inadequacy has been rectified by several measurement programs through the 1980s. Bennett et al. (1983), Fine and Molinari (1988), Bennett and McCartney (1990), Speer and McCartney (1991), and Molinari et al. (1992) all discuss hydrographic sections across the western boundary, with a

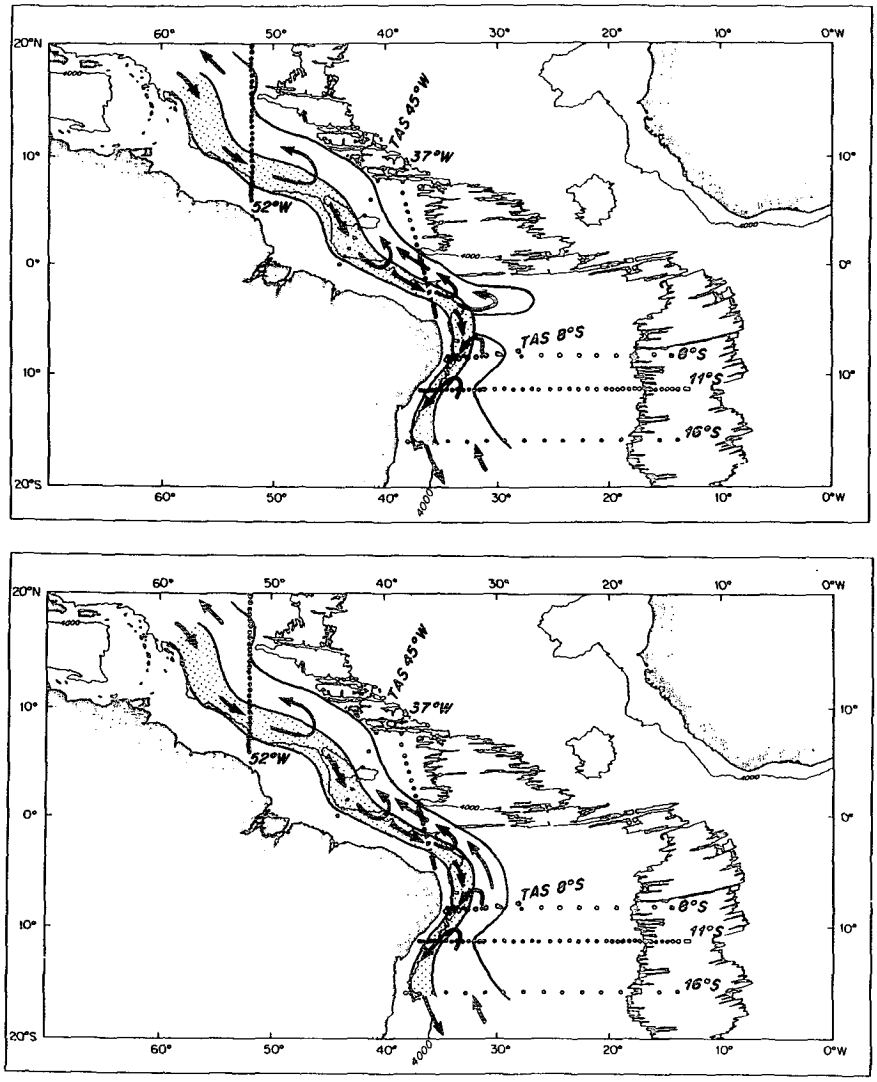

FIG. 2. Two extreme "models" of the deep circulation at and south of the equator: (a) An interpretation as two disconnected gyres, with a small transport DWBC bridging them. (b) An interpretation as connected gyres, with a large transport DWBC all along the boundary.

consensus emerging that the low-latitude North Atlantic DWBC transports on the order of 20 to 30 ($\times 10^6$ m^3 s^{-1}). Corroboration of these large transports is appearing in current meter velocity measurements (Johns et al. 1990, Johns et al. 1993; Leaman and Harris 1990; Lee et al. 1990). Deep float measurements are beginning to yield an image of the spatial field of flow (Richardson and Schmitz 1993).

Various studies of meridional heat flux (e.g., Hall and Bryden 1982) and North Atlantic general circulation (e.g., Wunsch and Grant 1982; Schmitz and McCartney 1993) agree in representing the meridional overturning cell that underlies the net poleward flux of heat at midlatitude as having net southward flow throughout the NADW to at least as warm as 4°C, and typically estimate the net southward transport of cold water of order 15×10^6 m^3 s^{-1}. The preceding DWBC transport estimates are distinctly larger than this net southward flow. The resolution of this transport disparity involves a gyre aspect to the flow of deep and bottom water in the low-latitude western basin of the North Atlantic, with the large southward transport of deep and bottom water in the DWBC partly canceled by the northward flow of deep and bottom water in the basin interior. The possibility of such recirculations was recognized by the authors listed in the preceding paragraph. The geostrophic signature of the recirculation is described in the present study, is also described by Friedrichs (1992), and is included in an overall North Atlantic circulation scheme by Schmitz and McCartney (1993). This Guiana abyssal gyre extends southward from the Guiana Basin across the equator

to the Pernambuco Abyssal Plain of the northern Brazil Basin. The deep water in the northward flowing limb of this gyre carries a southern influence into the North Atlantic; the tracer evidence for this northward flow has been commented on by Reid and Mantyla (1989), McCartney (1990), and Bennett and McCartney (1990).

Conventional geostrophic transport estimates cannot, of course, be made directly at the equator due to the degeneracy of the geostrophic relation as the Coriolis parameter goes to zero with latitude. McCartney and Curry (1993) take advantage of a topographic peculiarity of the western basin at the level of the AABW to make an equatorial geostrophic estimate of the transport of AABW as it flows westward along a zonal channel in the process of crossing the equator. Because of the topography, this westward transport of about 4 $\times 10^6$ m^3 s^{-1} is an estimate of the total flow of AABW from the Brazil Basin into the Guiana Basin. This method cannot be extended higher, into the NADW, for the topographic channeling does not reach much above 4000 m, nor is the characteristic isopycnal "bowl" or "dome" required for such a calculation in evidence in the NADW. Combining the import of 4 $\times 10^6$ m^3 s^{-1} of AABW into the North Atlantic with the order 15 $\times 10^6$ m^3 s^{-1} expected net export of cold water yields an indirect estimate of order 20 $\times 10^6$ m^3 s^{-1} for the net export of NADW from the North Atlantic. While the recognition of this opposing flow of AABW pushes upward the expected net flow of NADW, most of the DWBC transport estimates at low northern latitudes are even larger than this expected net flow, pointing to the possibility of other opposing flows or recirculations offshore of the DWBC.

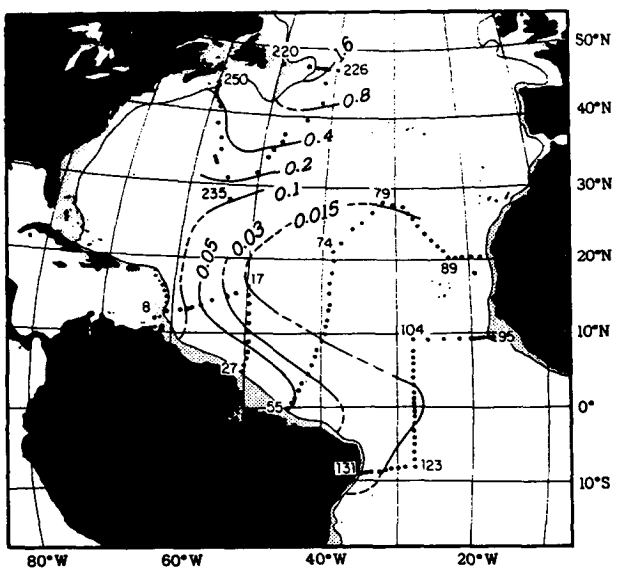

FIG. 3a. From Weiss et al. (1985), a chart of the distribution of the F11 CFC on the density surface $\sigma_{1.5}$ = 34.63 kg m^{-3}, with CFC concentrations in pmol kg^{-1}, and with successive contours above 0.5 pmol kg^{-1} representing a doubling of concentration.

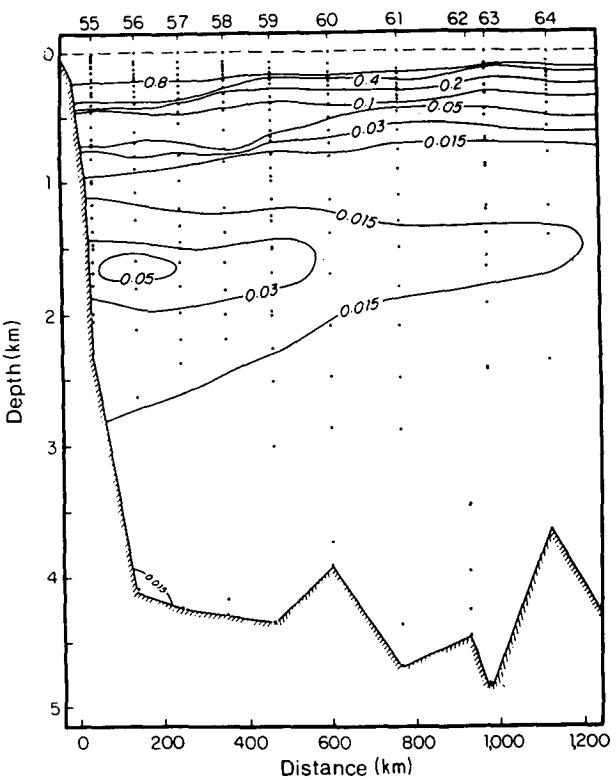

FIG. 3b. CFC (F11, pmol kg^{-1}) distribution along a quasi-meridional section near 40°W (south on left, after Weiss et al., 1985) made from the R/V *Knorr* in January 1983. Station positions are shown in Figs. 1 and 3a.

In the Stommel and Arons (1960) abyssal circulation framework, the low-latitude interior of a basin has only weak flow, and the circulation is completely dominated by the transequatorial transport of the DWBC. Besides the excess of DWBC transport, there are other indications that the tropical abyssal circulation may comprise more elements than just the DWBC. Charts by Wüst (1935) include dashed flow axes of upper and middle North Atlantic Deep Water (respectively, UNADW and MNADW) erupting from the western boundary and extending eastward near 5°S. A more immediate motivation for the study reported on here is a paper by Weiss et al. (1985) describing the distribution of chlorofluorocarbons (CFCs) in the UNADW in the North and tropical Atlantic. These measurements [and additional ones made a few years later (Weiss et al. 1989)] have been responsible for a surge of studies of the deep tropical Atlantic—observational, interpretational, and theoretical. The UNADW CFC (F-11) distribution that Weiss et al. charted with data from the early 1980s, Fig. 3, shows an image of western intensified UNADW suggestive of DWBC flow at low latitudes in the North Atlantic, but with the flow splitting at the equator into a southward continuation of

the DWBC into the South Atlantic, and an eastward flow along the equator. Weiss et al. (1989) have interpreted the evolving CFC distribution as showing the eastward flow intensity as larger than the continued southward flow of the DWBC. The present paper will describe flow elements missing from the interpretational framework they used, which probably voids their interpretation. In particular, it will be shown by geostrophic calculation that the DWBC of the Brazil Current is much more intense than any plausible along-equator flow.

In Fig. 3 CFC levels in the DWBC east of Newfoundland (in 1982–1983) were near 1.6 pmol kg^{-1}, with a 16-fold reduction indicated by 15°N, and a 30-fold reduction by the equator. Explicit in the quantitative interpretation of this field by Weiss et al. (1985) is the assumption of a DWBC filament in the North Atlantic bifurcating at the equator into two axes of flow. Their specific statement is that "the CFC distributions show that this western boundary flow crosses into the Southern Hemisphere to at least 9°S and suggest that the flow also extends eastward along the equator." Given this assumed basic advection, the decline in concentration along the DWBC and along the subsequent two axes reflects a combination of temporal variations (increase with time) of CFCs in the atmosphere of the northern source region reflected in the water mass source itself, the advection time from the source region to the point of observation, and the entrainment of other waters along that path.

Weiss et al. (1985) estimate that when allowance is made for the increase in CFC concentration with time at the source region for this particular stratum, the concentration at the equatorial location represents a fivefold dilution of source waters from circa 1960 by CFC-free water. Their calculation determines the age from the ratios of two CFCs, assuming the source water to be saturated at their atmospheric values and that the mixing is with CFC-free water, so that the ratio is preserved as the concentrations decline through mixing with the CFC-free water. The travel time of about 23 years from a Labrador Sea source to the equator indicates a mean speed of only 1.4 cm s^{-1}. Additional data later in the 1980s (Weiss et al. 1989, personal communication 1992) show continued eastward spreading of the CFC tongue along the equator and southward in the DWBC. They interpret these observations as indicating roughly the same time of origin (ca. 1960) as the earlier study, for both tongues, and a tenfold dilution. The eastward propagation speed along the equator is directly estimated as 2 cm s^{-1} from the zonal extension of the equatorial tongue between the two measurement periods, and similarly, a southward speed of 1 cm s^{-1} in the DWBC of the Brazil Basin is inferred.

The DWBC mean speed estimates seem low. If the 1.4 cm s^{-1} mean speed for the North Atlantic DWBC is assigned to a DWBC of dimensions 200-km width and 2500-m thickness, it would reflect a transport of only 7×10^6 m^3 s^{-1}, only about half the expected magnitude of the meridional overturning cell and about a quarter of the geostrophic estimates. The estimated speed of 1 cm s^{-1} for the low-latitude South Atlantic DWBC similarly yields a transport of only 5×10^6 m^3 s^{-1}, which is so small as to be essentially canceled by the northward flow of AABW beneath the NADW, thereby indicating essentially no net cold water transport! These low speeds are also troubling because the CFC speed estimate corresponds to a layer of the DWBC that is presumed more rapidly moving in some sense than the rest since it is the layer of strongest CFC concentration in the DWBC.

The methodology used by Weiss et al. (1985) and Weiss et al. (1989) for estimating of DWBC speeds has been demonstrated to cause systematic underestimation, with several processes complicating the interpretation now described in the literature. Wallace and Lazier (1988) observed recently formed Labrador Sea Water (LSW, which is essentially the same density as the CFC layer charted in Fig. 3) in the central Labrador Sea. Instead of CFC levels equal to those of the atmosphere in that particular year, as is usually assumed to be the surface boundary condition in interpretative studies, the observed concentration was only 60% of those levels, although the CFC ratio did match that of the atmosphere. They attribute this undersaturation to incomplete gas exchange due to the rapidity of convection compared to the order one month gas exchange time constant. This undersaturation would impact on the apparent dilution estimates downstream along the DWBC, though not on the age estimate (since the CFC ratio was preserved in spite of the lower concentrations). If the same degree of undersaturation existed in 1960, the time of origin inferred by Weiss et al. (1985, 1989), then their estimated degree of apparent dilution at the equator would be reduced from fivefold to threefold. Bullister and Weiss (1983) earlier reported what appears to be an analogous undersaturation of about 20% in the source region for denser components of the DWBC, the Nordic Seas, so uncertainty exists as to the surface boundary condition in the source region for all the DWBC components.

Pickart et al. (1989) describe two additional processes of importance, one for the source region, the other for the DWBC, both impacting on the interpretation of age as well as degree of dilution downstream along the DWBC. They recognized that the DWBC does not draw directly on surface water but rather that surface convection partially renews a reservoir of water from which the DWBC draws its source waters. Unless the residence time is very short, the source water will have CFC levels corresponding to an average of the surface value history rather than the instantaneous surface value, and the CFC ratio will not reflect an age in any simple fashion, since it will be the ratio of two time-averaged CFC values. For the known CFC history

for the atmosphere, the essentially monotonic increase in concentrations and CFC ratio, and assuming for the purpose of a sample calculation 100% saturation of the convecting waters, they show that the reservoir concentrations will always be lower than the atmospheric value for a given year (thus appearing undersaturated) and will always have a smaller CFC ratio than the overlying atmosphere (thus appearing to have nonzero age). Their specific example used the semienclosed basin of the Nordic Seas that is the source reservoir of the denser levels of the DWBC. The same concept can be extended to the cyclonic recirculating gyre of the Labrador Sea as a reservoir within which the convection produces new LSW and out of which the upper levels of the DWBC draw their source waters.

The other process examined by Pickart et al. is self-mixing of CFCs as the DWBC evolves in time. The DWBC rapidly advects source waters along the boundary, but only at the very beginning of CFC input is dilution achieved by mixing with CFC-free interior. Subsequently, the mixing occurs through a layer of CFC that exists because of the prior accumulation of CFCs by the time integral of diffusion from the DWBC into its surroundings. They consider two models for the DWBC, the first a constant speed slug flow with a quiescent surrounding fluid, the second replacing the slug with a two-speed representation of shear in the DWBC: a high speed core with a slower speed regime between the core and the quiescent surrounding fluid. In this latter case the high speed core (younger water with higher CFC concentrations and higher CFC ratio) is mixing with older waters in the slower regime (lower concentrations and lower CFC ratio), which in turn is diffusing CFC into a surrounding boundary layer with still older accumulated average CFC characteristics. In sample calculations for these two advection models the modification of core CFCs by the mixing causes the apparent speeds (as deduced from core CFC ratio) to underestimate core speed. Combining these DWBC representations with the source reservoir effect gives net speed underestimates of factors between 2 and 5 for their sample calculations (the Iceland–Faroe overflow level of the system, over about a 9000-km pathway from the overflows to the region south of Newfoundland). To my knowledge a similar calculation has not been made for the LSW level of the DWBC system, represented by the distribution of Fig. 3, to evaluate the explicit impact of replacing the Weiss et al. (1985) and Weiss et al. (1989) simple interpretational framework with a more realistic treatment of source conditions and the DWBC advective–diffusive structure.

In the subsequent sections of this paper a fourth process affecting CFC distributions will be revealed. The deep circulation at lower latitudes is not well represented by a DWBC filament penetrating an essentially motionless interior. Instead the DWBC transport is boosted by western-intensified deep recirculating gyre flow. For this system a more appropriate advection field would have a DWBC comprising both northern source waters and recirculating flow from the interior, and a somewhat broader opposing flow representing the recirculation of deep water back north offshore of the DWBC. It is anticipated that using this more realistic advection field will result in significantly different speed and dilution estimates for the arrival at the equator of the DWBC and the continued southward penetration into the Brazil Basin than the simpler model used by Weiss et al. (1985) and Weiss et al. (1989).

The CFC extrusion along the equator (Fig. 3) is intriguing, and has led to theoretical studies into the cause of the DWBC apparently bifurcating with an eastward branch along the equator. Kawase (1987) examined the evolution and steady state of a two-layer abyssal circulation model, where the upwelling velocity is not prescribed as in the Stommel and Arons (1960) theory, but instead is proportional through a damping coefficient to the departure of the interface from its equilibrium depth (and with DWBC structure determined by a Rayleigh friction parameterization in each layer). When the damping is small, an analog to the Stommel and Arons solution is obtained, with the DWBC crossing the equator and continuing on as a DWBC in the Southern Hemisphere. For large damping, the DWBC finds the equator a barrier, and turns offshore as a jet along the equator. Rothstein et al. (1991, personal communication) indicate that this range of behavior is not a function of the damping parameterization, but can also occur in more traditional vertical mixing parameterizations. However, the branching out along the equator only occurs for unrealistically large vertical diffusivity. For diffusivity in the expected oceanographic range, the cross-equatorial DWBC flow is dominant.

Kawase et al. (1992), using a very high resolution numerical model, conclude that a steady-state DWBC flow bifurcating with a significant alongequator branch cannot occur. They comment that this conclusion appears at odds with the CFC distribution, and in attempting to sort out the difference make two points. The first is that "the tracer distribution is likely to be a poor indicator of the mass transport." This is, of course, a familiar caution, with the relation of tracer tongues to the advection field always being problematic when the advection is not directly measured. Their particular demonstration is taken from the end of their model run, when the system is approaching a steady state. There is a small residue velocity along the equator, which, although negligible in speed and transport compared to the DWBC flow, has speed larger than the background interior flow into which it moves. Thus, it could provide an advection axis generating a property tongue contrasting with the background of the interior, in spite of being a small transport element compared to the DWBC. Their model's weak along-equator speed is on the same order as that inferred by Weiss et al. (1989) from comparisons of 1988 equatorial data to that of Fig. 3, about 2 cm s^{-1}. Their second point is

that the model shows DWBC speeds an order of magnitude larger than the along-equator speeds, while the Weiss et al. (1989) CFC-inferred DWBC advection speed is actually half that of the inferred alongequator speed. They conclude that there appears therefore to be a fundamental difference between the model circulation and the circulation inferred from the time evolution of the oceanic CFC distribution. These model results find support in the present study's real ocean data: the actual oceanic circulation near the western boundary has much larger speeds than those estimated from CFC distributions, and there are other elements in the low-latitude circulation whose action is to dilute the tracer levels in the DWBC and to cause the CFC concentrations to decline steeply along the DWBC. These elements do not appear in the numerical model, so their physics remains unknown.

The Kawase et al. (1992) model runs are highly resolved in the vertical, 50 levels. The equatorial structure of the solutions does not exhibit the multiple along-equator jets of an earlier set of studies by Suginohara and coworkers (Suginohara and Fukasawa 1988; Suginohara and Aoki 1991; and Suginohara et al. 1991) with lower vertical resolution. This seems to support the interpretation by Weaver and Sarachik (1990, 1991) that these reversing jets, and the accompanying reversing transequatorial flows, are computational modes rather than physically realistic phenomena. On the other hand, there are measurements on the equator (Ponte et al. 1990) that show layered reversing jets in the NADW near 30°W, with eastward flow at the level where Weiss et al. (1985) charted the CFC maximum layer. The relation of this instantaneous velocity profile to the time-mean flow is not known.

3. The crossing of the equator by the DWBC and estimation of its NADW transport

The present paper's contribution to the interpretation of the CFC distribution comes from the quantification of the DWBC transport at three locations in the tropical Atlantic. Two are in the Brazil Basin, one immediately south of the equator and the other near 11°S, and the third is near 6°N in the Guiana Basin. The large southward transport of the DWBC observed at these three locations is partly balanced by a northward recirculation of deep water. This recirculation will be quantified at the 6°N and 11°S locations, but it falls at the equator for the third section, and although visible in property distributions, cannot be quantified due to the degeneracy of geostrophy at the equator. One gyre recirculation centers over the Guiana Abyssal Plain of the Guiana Basin north of the equator, but penetrates the equator to the Pernambuco Abyssal Plain of the northern Brazil Basin, while another appears in the 11°S section and has incompletely documented geography. The degree of linkage of these two recirculations cannot be established with presently available data, thus the range of circulation extremes shown in Fig. 2. The combined action of these circulation elements on the NADW is to dilute the northern source component in the DWBC with interior waters. More extreme dilution occurs for the UNADW, for most of its DWBC flow occurs beneath the counterflowing AAIW within the North Brazil Current. Diapycnal downgradient fluxes between the counterflowing AAIW and UNADW cause mutual erosion. We will use the traditional water mass tracers, dissolved oxygen and nutrients, to illustrate this dilution, as they are the tracers measured on these 1983 sections, made within a year after the tropical data of Fig. 3.

Property distributions along the tropical portion of a section near 37°W are shown in Fig. 4. The cold AABW is flowing westward through a channel centered at the equator with a transport of about 4.3×10^6 $m^3 s^{-1}$ according to McCartney and Curry (1993), and close to the 4.0×10^6 $m^3 s^{-1}$ estimated at 4°N by McCartney (1993). East of the section the AABW flows northward from the Brazil Basin into the channel, flows westward along the channel, and exits northwards from the channel into the Guiana Basin west of the section. South of the equatorial channel over the continental slope of Brazil, isotherms[1] between 2° and 3.8°C (Fig. 4a) rise toward the western boundary (the southern end of the section). This is the shear signature[2] of the DWBC flow of NADW. In the South Atlantic the deep circulation can be quantified by choosing a reference level that is a level of no motion (LNM) between the NADW and the AABW, or at the bottom at locations where there is no AABW (Wright 1970; Hogg et al. 1982). This traditional LNM choice in the South Atlantic reflects the necessity of net flow away from the sources for these two water masses, and the assumption that the net flow constraint can be applied to the individual flow components of a given section. When both water masses are found in the DWBC, for example, in the 11°S section discussed later in section 6, this assumption appears reasonable, as both water masses exhibit western intensification of their characteristics. For the 37°W section this traditional choice corresponds over the continental slope to choosing the bottom as an LNM, and this converts the shear implied by the southward rise of isotherms and isopycnals into an eastward flow increasing upwards to a maximum speed near 4°C, where the isopycnals reverse slope. The reversed shear above the speed max-

[1] All temperatures in this paper are potential temperatures.

[2] Isopycnals, shown in Fig. 4b, are close to parallel to isotherms below 4°C, so the sense of the deep shear is adequately deduced by the isotherm distribution. Most readers are likely to register more easily on temperatures when discussing water masses, so temperature will be used when appropriate (below about 4°C) as a proxy for density in the following discussion.

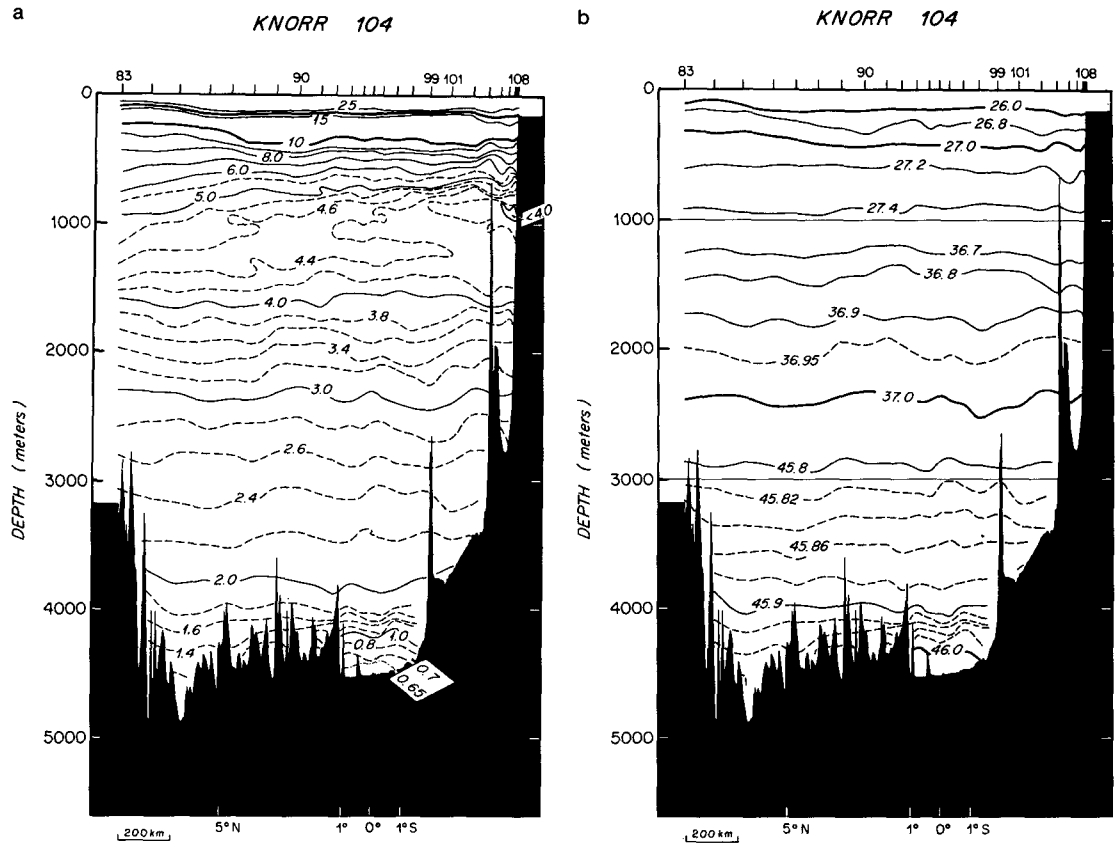

FIG. 4. Property distributions along a quasi-meridional section near 37°W (south on right) made from the R/V *Knorr* in August 1983. Station positions are shown in Fig. 1. (a) Potential temperature (°C). (b) Potential density anomaly (EOS80, kg m^{-3}). (c) Dissolved oxygen (ml l^{-1}). (d) Silicate (μmol l^{-1}). (e) Nitrate (μmol l^{-1}). (f) Salinity (psu).

imum leads to westward flow at shallow levels—the North Brazil Current.

Confirmation that the southern deep shear region is indeed the DWBC is found in the tracer sections. The oxygen distribution (Fig. 4c) shows the lower NADW characterized by an oxygen maximum defined by the 6.0 ml l^{-1} contour and that this contour abruptly expands between stations 98 and 99 from warmest associated temperatures of about 2.1°C near 3500 m in the equatorial channel to about 3.1°C near 2200 m in the southern stations. The stronger northern source influence thus is found at stations 99–105, the group defining the DWBC shear. Offshore (north) of the DWBC, the lower NADW temperature range is characterized by lower oxygens than within the DWBC, with a stack of weak extrema centered on the equator. The silicate distribution (Fig. 4d) shows a similar contrast of silicate along isotherms, with lower silicate values at and south of station 98 compared to at and north of station 97. Particularly striking is the "cat's eyes" silicate maximum layer centered on the equator near a temperature of 2.3°C. A related pattern is recognized in the nitrate distribution (Fig. 4e): lower values in the DWBC and a deep-water regime with a stack of weak extrema centered on the equator. These patterns have been interpreted as deep water from the low latitudes of the Brazil Basin flowing to the Guiana Basin in parallel with the AABW below, as part of the Guiana abyssal gyre (McCartney 1990), and will be further discussed in the next section.

As noted in the background section, the deep water in the equatorial channel of the 37°W section (Fig. 4) is not amenable to equatorial geostrophic estimation of its transport—nor to conventional geostrophic estimation. The DWBC transport immediately south of the equator can be estimated, but the geostrophic calculation is less certain than normal for two reasons. First, slight station-to-station residual uncertainties of calibrations for the CTD data, while not particularly troublesome at midlatitudes, become problematic as geostrophic estimates are made closer to the equator. This is because the shear is inversely proportional to the diminishing Coriolis parameter, amplifying the impact of the density uncertainty on the calculation of shear. Second, the differential form of the geostrophic relationship has the dynamic height gradient divided by the Coriolis parameter, and the conventional midlatitude finite-difference approximation for this uses

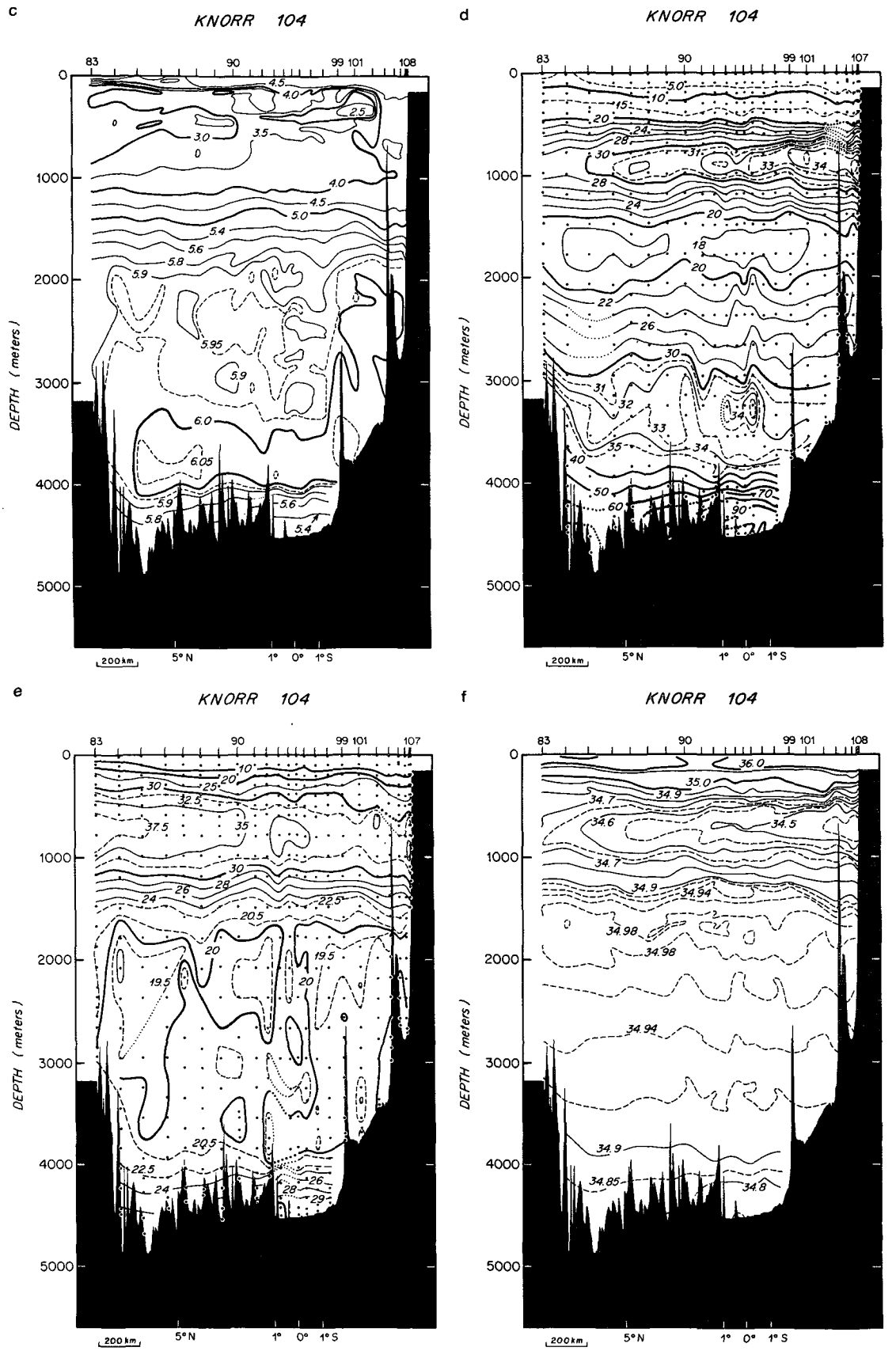

FIG. 4. (*Continued*)

the mean latitude of a pair of stations to calculate a mean Coriolis parameter to divide into the dynamic height difference between the two stations. This is not a valid approximation close to the equator, but this nuance will be ignored in the present study.

For all the transport calculations in this paper a definition for NADW will be needed. Comparison of the oxygen and temperature sections (Figs. 4c and 4a) shows the high oxygen northern source influence to be limited from below by the transition to lower oxygen AABW, colder than about 1.8°C. In the DWBC regime south of station 98, the influence is limited from above by the transition to lower oxygen AAIW, warmer than about 4°C, with the transition layer generally called Upper Circumpolar Deep Water (UCDW). Defining an upper boundary to the NADW thus involves an ad hoc choice of some level in this transition, which is taken as the $\sigma_2 = 36.65$ surface, midway through the transition, with associated temperatures near 4.3°C. The bottom will be defined by the $\sigma_2 = 37.10$ surface, in the transition layer from LNADW to AABW with associated temperatures near 1.9°C at this section. The associated temperatures of these two densities will be slightly different at the other two DWBC locations along the western boundary subsequently discussed.

The DWBC is taken as the station group with the thick high oxygen influence, stations 99 and southward. For the geostrophic calculation station 98 is included as station pair 98–99 defines the transition to lower oxygen as occurring between this pair, and isopycnals reach a maximum depth at station 98 defining that station as the offshore edge of the DWBC shear signature. For this station pair the bottom of the NADW is used as the LNM, while to the south the seafloor is used. The resulting geostrophic estimate is 35.2×10^6 $m^3\ s^{-1}$ eastward transport of NADW in the DWBC at nominally 3°S, 37°W. The proximity of this section to the western boundary intersection with the equator indicates that this estimate should be regarded as a direct estimate of the transequatorial transport of NADW from the Guiana Basin to the Brazil Basin.

The use of the traditional LNM at this location can be defended. Figure 5 illustrates the dependence of the estimated DWBC transport of NADW on the assumed LNM, with transports of subdivisions of NADW also shown to aid the discussion. As the LNM is raised to progressively lighter density levels, the total NADW transport initially rises somewhat to a maximum of about 39×10^6 $m^3\ s^{-1}$ for an LNM near 3000 meters, then steeply declines to reverse to westward transport for LNMs shallower than about 2500 meters. The larger net transports have the NADW subdivisions all transporting westward. The decline in net transport for the shallower LNMs is achieved by reversing the net transport of LNADW to westward, which is inconsistent with the DWBC LNADW characteristics showing strong northern source influence. Further elevation of the LNM progressively reverses the MNADW and

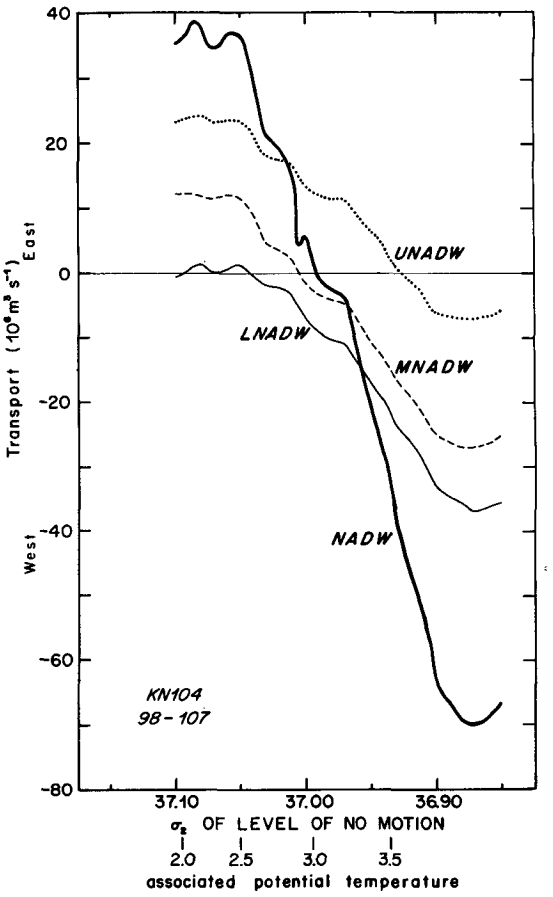

FIG. 5. Transports (10^6 $m^3\ s^{-1}$) of NADW and NADW components in the DWBC near 3°S, 37°W in the northern Brazil Basin as a function of the density of the assumed level of no motion. NADW defined as layer between $\sigma_2 = 37.1$ and 36.65, and divided into lower, middle, and upper components (LNADW, MNADW, and UNADW) by $\sigma_2 = 37.04$ and 37.95.

UNADW transports from eastward to westward. The deep LNM is thus the most plausible choice.

The transport estimate of 35×10^6 $m^3\ s^{-1}$ transequatorial NADW transport in the DWBC is large compared to the conventional estimate of a net meridional overturning cell of order 15×10^6 $m^3\ s^{-1}$ (for a net cold water transport of order 20×10^6 $m^3\ s^{-1}$ when the opposing transport of 4×10^6 $m^3\ s^{-1}$ AABW is allowed for). The DWBC transport estimate is also larger than an average (for 14 DWBC crossings) NADW transport of 23.7×10^6 $m^3\ s^{-1}$ reported by Molinari et al. (1992) for the low-latitude North Atlantic between 15° and 5°N.[3] It is within the range 26

[3] They use 1.8°C and 4.7°C to define the NADW layer, so the estimates are not directly comparable to the present density-defined layer. Temperature structure between 3.7° and 5.0°C is very convoluted in the NADW–AAIW transition for the present paper's sections, so the σ_2-based NADW definition will be used hereafter.

to 35 ($\times 10^6$ m^3 s^{-1}) at 8°N described in the next section. But it is smaller than estimates between 40 and 50 $\times$ 10^6 m^3 s^{-1} for the DWBC at 11°S in the Brazil Basin discussed in section 6.

4. A gyre component to the transequatorial deep water flow

North of the equator the resolution of the disparity between the DWBC transport and the expected net cold water transport of the meridional overturning cell has been revealed by property distributions and geostrophic shear as a pattern of northward transport through the interior of the Guiana Basin. This flow represents a recirculation back northward of part of the transport of the DWBC and together with the DWBC the flow field is a Guiana abyssal gyre (Bennett and McCartney 1990; Friedrichs 1992; Schmitz and McCartney 1993). The gyre "center" is over the Guiana Abyssal Plain, and has counterclockwise (cyclonic north of the equator) circulating NADW and AABW. The DWBC transport is boosted by the western limb of the gyre, but a smaller net southward transport results because of compensation by the northward interior flow offshore of the DWBC.

Figure 6 shows property distributions along the tropical portion of a section near 52°W to illustrate the DWBC and recirculation signatures in shear and deep water mass characteristics. NADW and AABW isotherms and isopycnals rise southward from near 10°N to the western boundary near 7°N (except for some reversals in the extreme south over the Demerara Plateau at 7°–7.5°N). This is the DWBC carrying the most extreme NADW (high oxygen, low silicate and nitrate, and most intense salinity maximum) toward the South Atlantic, and also recirculating southeastward cold AABW, which flows northwest in the basin interior. At this section, the gyre center is near 10°N, and between there and 14°N, the overall northward rise of NADW and AABW isotherms and isopycnals is the shear signature of the poleward (northwestward) flowing limb of the gyre. This limb brings the AABW from the equator into the central North Atlantic, and recirculates back towards its source part of the NADW (from the DWBC) with less extreme NADW characteristics (diminished oxygen, elevated silicate and nitrate, and diminished salinity maximum). Above all this, the AAIW distribution suggests the opposite rotation with western boundary current flow bringing AAIW westward in the south, and an interior recirculation carrying diluted AAIW back eastward.

Consistency between the property distributions and the field of flow calculated from the geostrophic shear leads to choosing a LNM in the Guiana Basin at a level above the NADW. Using the top of that layer, σ_2 = 36.65, as a first try for an LNM and keeping in mind the ad hoc nature of that choice for the top, this section yields a DWBC (stations 211–227) transport of NADW to the east of 26.5 $\times$ 10^6 m^3 s^{-1}, accompanied by 10.7 $\times$ 10^6 m^3 s^{-1} of AABW ($\sigma_2 \geqslant 37.1$, approximately 1.95°C at 52°W). This net DWBC cold water transport of 37.2 $\times$ 10^6 m^3 s^{-1} is partially compensated by the westward transport of the opposing limb[4] (stations 227–233) of the gyre: a net of 27.8 $\times$ 10^6 m^3 s^{-1} comprising 16.7 $\times$ 10^6 m^3 s^{-1} of NADW and 11.1 $\times$ 10^6 m^3 s^{-1} of AABW. Thus, the net flows through the gyre for this LNM are an eastward transport of 9.8 $\times$ 10^6 m^3 s^{-1} of NADW, a westward transport of 0.4 $\times$ 10^6 m^3 s^{-1} of AABW, and thus a net eastward transport of cold water amounting to 9.4 $\times$ 10^6 m^3 s^{-1}. A net westward flow of 12.0 $\times$ 10^6 m^3 s^{-1} AAIW concentrated south of station 221 occurs above the NADW.

These estimates are very sensitive as to the placement of the LNM in the transition layer between the UNADW and the AAIW, as there is strong vertical shear in the layer. For example, elevating the LNM about 150 m to σ_2 = 36.55 increases the cold water transport of the DWBC to 44.9 $\times$ 10^6 m^3 s^{-1} (35.2 $\times$ 10^6 m^3 s^{-1} of NADW) and of the gyre net cold water transport to 14.6 $\times$ 10^6 m^3 s^{-1}, comprising net eastward NADW flow of 16.5 $\times$ 10^6 m^3 s^{-1} and net westward AABW flow of 1.9 $\times$ 10^6 m^3 s^{-1}. With this LNM the net westward flow of AAIW is 8.0 $\times$ 10^6 m^3 s^{-1}, mostly south of station 221, where its core layers are strongest. As before, these estimates are not intended to be definitive.[5] They show that it is likely that the net meridional overturning mode of the North Atlantic of order 15 $\times$ 10^6 m^3 s^{-1} is likely achieved principally as a net flow through a western-intensified cyclonic gyre whose limbs transport order 35 $\times$ 10^6 m^3 s^{-1} southward and 20 $\times$ 10^6 m^3 s^{-1} northward. Friedrichs (1992) also describes this gyre, from other data, with the gyre limbs transporting 29 and 14 ($\times 10^{16}$ m^3 s^{-1}) of NADW.

The part of the Guiana abyssal gyre west of 50°W and north of 10°N appeared on one of the data inversion charts by Wunsch and Grant (1982, their Fig. 16a) but was not mentioned in their discussions. The precursor to their paper by Wunsch (1978) also showed the northern part of this "southern gyre," and noted its absence in earlier North Atlantic circulation schemes.

---

[4] There are property isopleth reversals between stations 233 and 235, recovering between 235 and 240. These smear the signature of the northern edge of the gyre and seem to reflect its interaction with the rough foothills of the Mid-Atlantic Ridge north of 15°N. The silicate section (Fig. 5d) shows by the shape of the 36 and 38 μmole l^{-1} contours that the recirculation of LNADW appears limited to south of station 233, except for an isolated "blob" at station 235.

[5] I am inclined toward the 36.55 LNM and its resulting larger DWBC and gyre transports because the net AABW transport of 1.9 $\times$ 10^6 m^3 s^{-1} that LNM yields fits in with an estimated 4.0 $\times$ 10^6 m^3 s^{-1} of AABW crossing 4°N in the southern Guiana Basin (McCartney 1993) having about 2.2 $\times$ 10^6 m^3 s^{-1} diverted to the eastern basin through the Vema Fracture Zone at 11°N (McCartney et al. 1991).

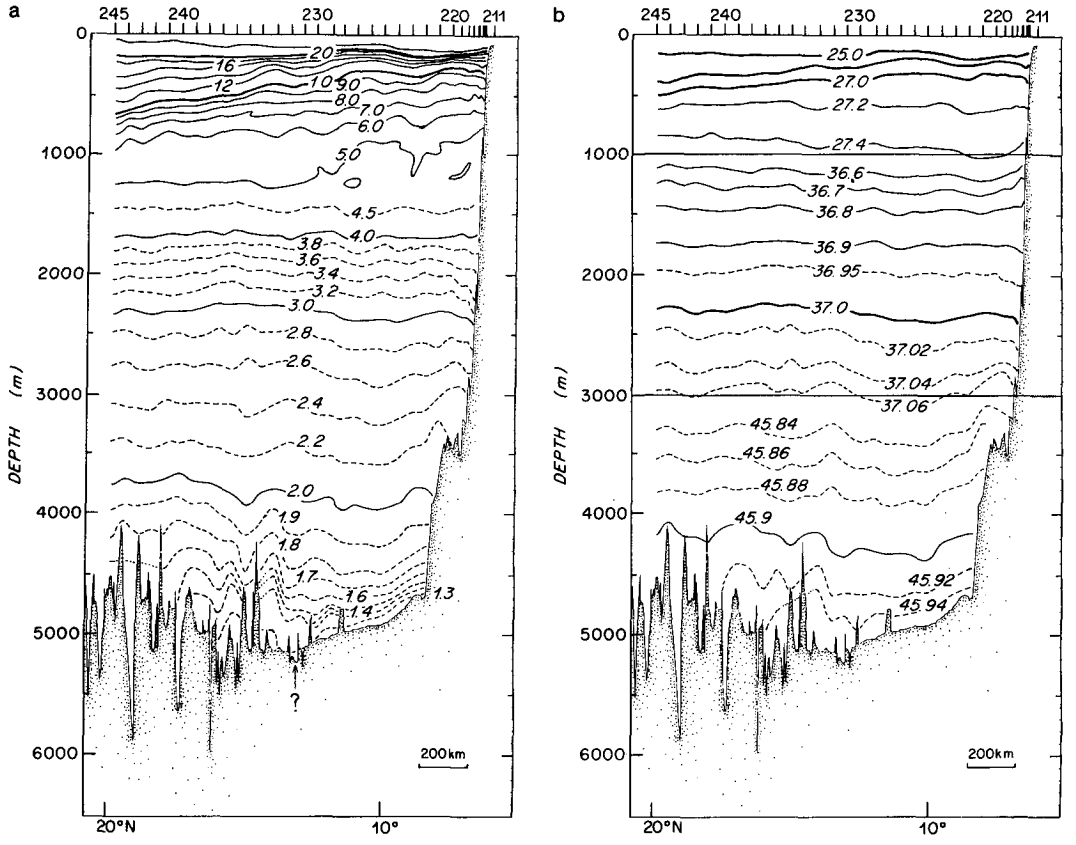

FIG. 6. Property distributions along a quasi-meridional section near 52°W (south on right) made from the R/V *Oceanus* in May 1983. Station positions are shown on Fig. 1. From Knapp and Stommel (1985). (a) Potential temperature (°C). (b) Potential density anomaly (EOS80, kg m^{-3}). (c) Dissolved oxygen (ml l^{-1}). (d) Silicate (μmol l^{-1}). (e) Nitrate (μmol l^{-1}). (f) Salinity (psu).

In the AABW the gyre appears to close over the Para Abyssal Plain near 5°N, for there is little indication for cold AABW in the DWBC between there and the equator in the NODC data archive. The closure may be related to the blocking effect of the Ceara Rise. At the equator in the 37°W section (Fig. 4) the AABW flow appears unidirectional from the South Atlantic to the North Atlantic (McCartney and Curry 1993). In the NADW, however, the gyre appears to close at low latitudes in the South Atlantic, over the Pernambuco Abyssal Plain, so that a counterflow exists across the equator: the DWBC carrying NADW southward with stronger northern source character than the return flow with its larger southern dilution. It is this south-to-north deep-water flow that is responsible for the silicate cat's eyes and other South Atlantic water mass characteristics over the equatorial channel at 37°W (Fig. 4), and these inversions and structures persist well north, being visible in the 52°W section (Fig. 6). Reid and Mantyla (1989) have inferred a flow of deep water from the South Atlantic to the North Atlantic from the slightly lower salinity of the deep water of the Southern Hemisphere compared to that in the DWBC; Bennett and McCartney (1990) and McCartney (1990) have described the water mass and shear signatures of this south-to-north flow of deep water. While these property distributions show the existence of deep water flow from the Brazil Basin to the Guiana Basin, its intensity at the equator unfortunately cannot be directly quantified from geostrophic calculations.

5. Circulation elements affecting the UNADW characteristics

The Guiana abyssal gyre flow, with transequatorial components, can be thought of as meridionally displacing and elongating the interaction between northern and southern varieties of deep water. Mixing between the two opposing flows and the recirculation's convergence and divergence of flow lines into and out of the DWBC cause more rapid dilution of the northern source influence within the DWBC than would occur if the DWBC flow were adjacent to a relatively motionless interior. In other words, the DWBC is larger in transport because of the recirculating component and lower in average northern source content because of the Southern Hemisphere influence that recirculat-

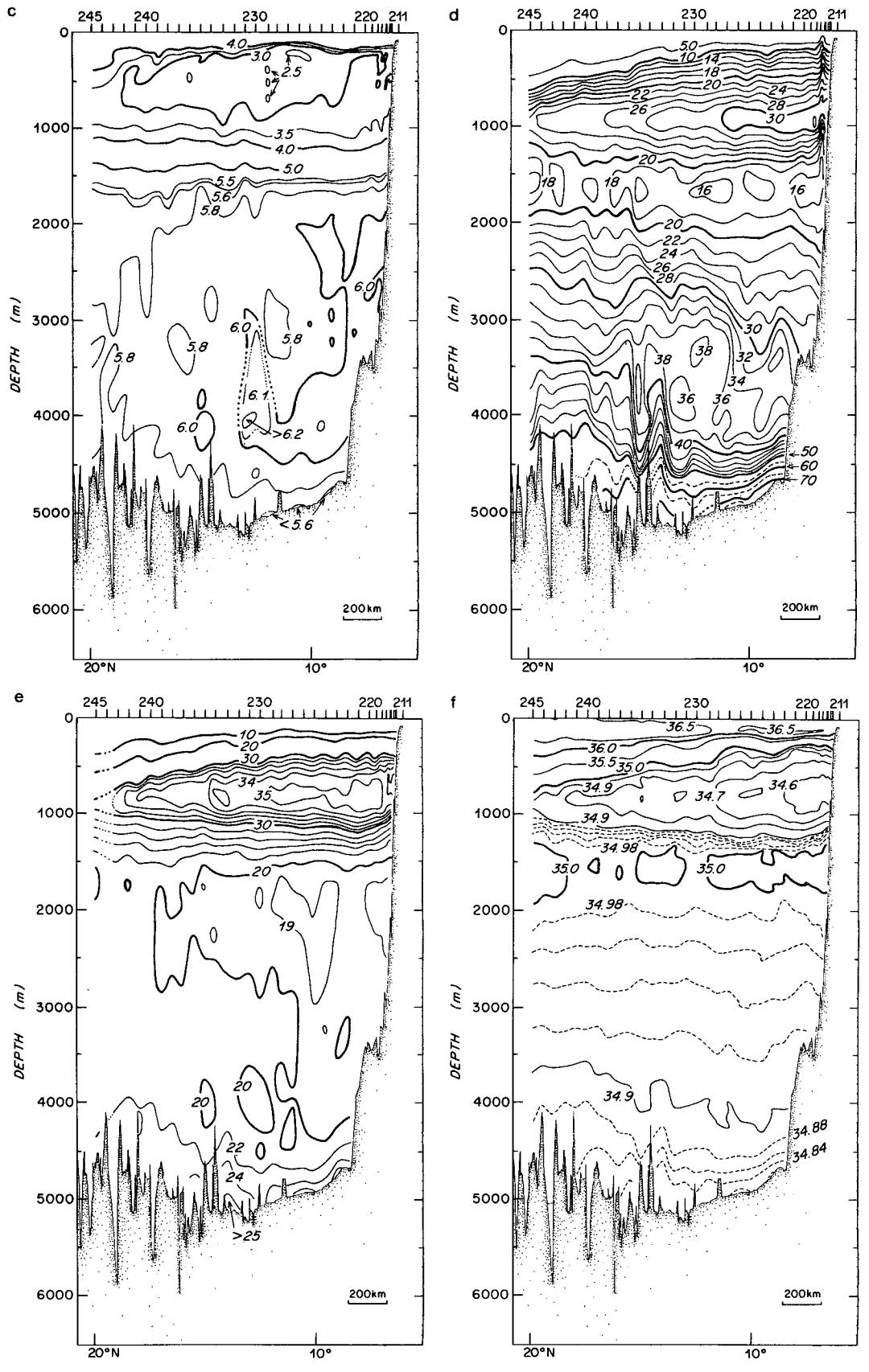

FIG. 6. (*Continued*)

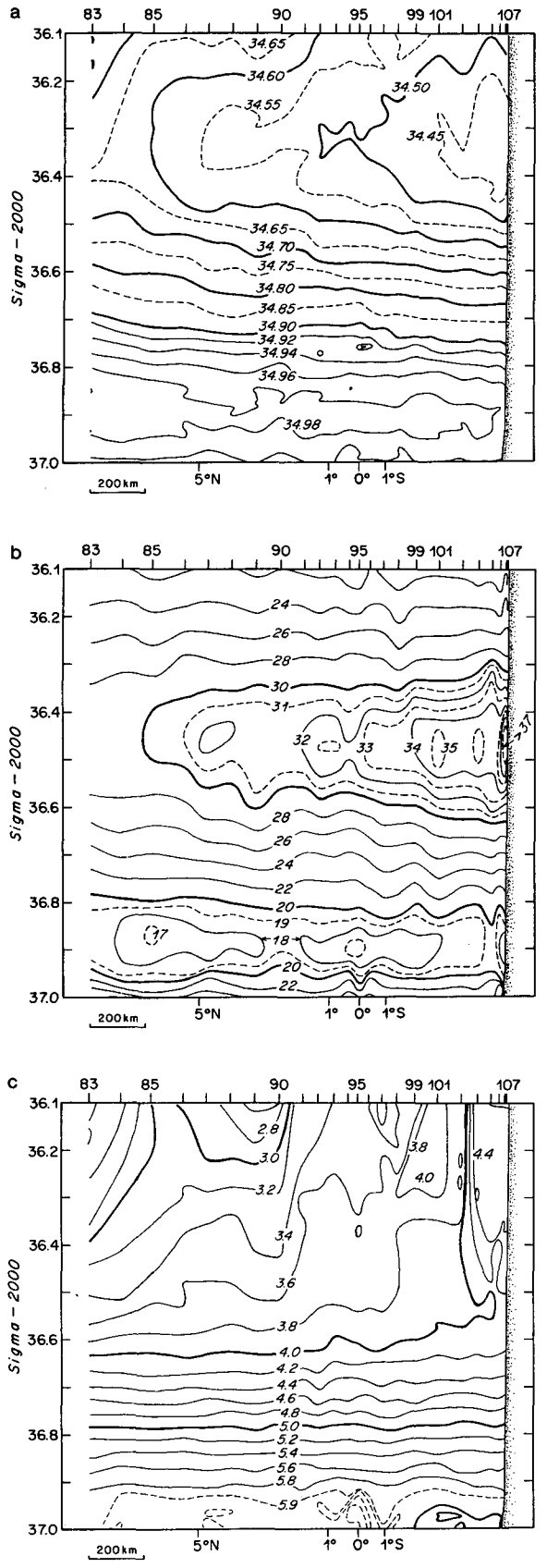

ing component acquired in the south and returns northward in the eastern limb of the gyre. This is part of the reason why the DWBC core CFC values in Fig. 3 decline so steeply with decreasing northern latitude between 12°N and the equator.

The existence of the recirculating component also leads to a different interpretation of the width of the low-latitude CFC tongue (and of other tracers like salinity and oxygen as charted by Wüst 1935). The width does not reflect a diffusional boundary layer adjacent to a southward flowing DWBC penetrating a quiescent interior, but rather the width of the recirculation of the Guiana abyssal gyre, a southward flowing DWBC with higher CFC than the northward flowing offshore limb of the gyre, with CFC-free water only farther offshore. Figure 3b reprints the section of CFCs from the Weiss et al. (1985) study. The section is nearly meridional near 45°W (see the CFC chart of Fig. 3a and the station chart of Fig. 1), with the southern station just 10 km north of the equator and halfway up the continental slope at the western boundary. The highest CFC value in the UNADW is one station removed from the western boundary, although this may not be significant given the ±0.005 pmol kg^{-1} limit of replicate analyses and given that other UNADW tracers (silicate minimum, salinity maximum) are strongest at station 55. While the highest CFC values are concentrated at the southern three stations, the 0.03 pmol kg^{-1} contour extends north past station 59, and the 0.015 pmol kg^{-1} contour all the way across the section to the Mid-Atlantic Ridge. This scale is similar to the gyre scale in Fig. 6. It thus appears that the CFC layer in the UNADW described by Weiss et al. (1985) spans both limbs of the gyre, with maximum concentration in the return flow of order 25%–50% of that in the DWBC. A similar relationship between the CFC distribution and the gyre shear field is inferred to the north since the present 52°W section (Fig. 6) shows the gyre center near 10°N, which on Fig. 3 falls near the 0.05 pmol kg^{-1} contour. The nearest data control for this CFC contour is the Tropical Atlantic Study section along 50°W. That section's temperature and density distributions [not shown, data reported by Scripps Institution of Oceanography (1986)] reveal deep isopleth bowls similar to those at 52°W (Fig. 6) centered between 7.6°N and 9.0°N, bracketing the 0.05 pmol kg^{-1} contour on Fig. 3.

In the lower part of the NADW, between 2° and 3°C, Fig. 6 shows that the Guiana abyssal gyre is about twice the width of the DWBC. In this wider gyre-scale

FIG. 7. Property distributions along a quasi-meridional section near 37°W (south on right) made from the R/V *Knorr* in August 1983. These are plotted with σ_2 as a vertical coordinate for a limited range spanning the core layers for the AAIW and the UNADW. Station positions are shown in Fig. 1. (a) Salinity (psu). (b) Silicate (μmol l^{-1}). (c) Oxygen (ml l^{-1}).

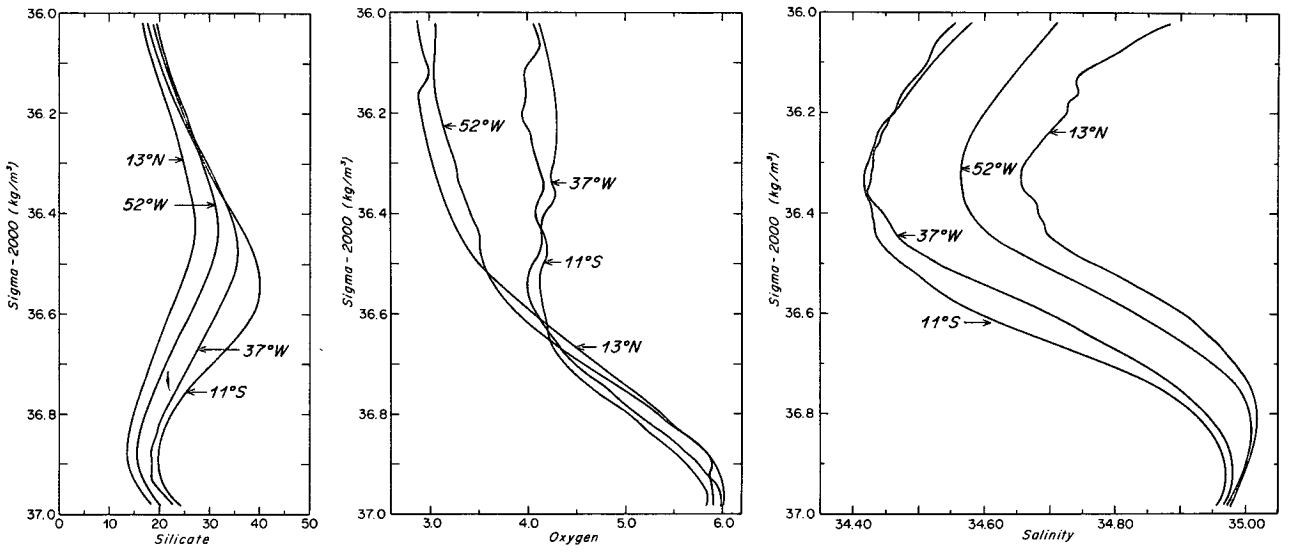

FIG. 8. Potential density (σ_2)–property relations for stations at the core of the DWBC for the UNADW and AAIW. Station positions are shown in Fig. 1. (a) σ_2–Silicate. (b) σ_2–Oxygen. (c) σ_2–Salinity.

band adjacent to the western boundary, NADW characteristics are more extreme than farther offshore, while within the band the NADW is more extreme in the DWBC than in the gyre return flow. In the classic NADW distribution charts of Wüst (1935) it is the wider band that dominates the image of western intensification of the NADW because of the limited sampling of the DWBC by his stations. In the North Atlantic part of the UNADW CFC distribution (Fig. 3), as just discussed, this same wider band appears, a modern analog to Wüst's charts.

There is another circulation element that affects the property distribution of the UNADW (but not the MNADW or LNADW). Property–depth profiles by Weiss et al. (1985) show that the CFC core coincides with the silicate minimum and the salinity maximum, with the latter being Wüst's (1935) definition of the UNADW core. Along the 37°W section (Fig. 4) the core layer distributions through the NADW show a shift in pattern with depth. Below about 2000 m, as described above, the NADW properties are southern-intensified with characteristic higher oxygen and low nutrients associated with the geostrophic signature of the DWBC. On the other hand, the silicate minimum and salinity maximum layers of the UNADW, centered near 1800 meters, show the strongest northern source influence over the equatorial channel rather than being southward intensified. This would seem to be the image in classical tracers of the pattern of CFCs (Fig. 3) showing a concentration along the equator rather than to the south at the western boundary. One interpretation of this UNADW pattern (the shear at and near the equator cannot be calculated to confirm or deny it) is that the principal axis of flow of UNADW is shifted offshore relative to the rest of the NADW, that is, that the axis of maximum core layer signal coincides with the principal flow axis. This interpretation is implicit in describing Fig. 3 as showing the DWBC splitting at the equator. There is, however, a different interpretation, which is developed next.

In the southern part of the 37°W section (Fig. 4) there is a distinct layering of water masses. The southward-intensified salinity minimum core layer of the AAIW lies near 800 m, with associated oxygen values higher than offshore, and is most concentrated at stations 102–108. An associated silicate maximum layer is somewhat deeper, near 900 m, has an associated minimum in oxygen and seems somewhat broader, stations 99–107. This could more properly be considered as a UCDW core layer, but for the present purpose it is adequate to call it part of an AAIW layer with southern sources. These AAIW signatures are associated with the deeper levels of the westward flow of the North Brazil Current, appearing to penetrate to about 1000 m, and flowing counter to the DWBC below. If the AAIW layer is coarsely defined as σ_2 between 36.0 and 36.65 (the top of the NADW), and $\sigma_2 = 37.1$ or the bottom is used as an LNM, then the westward transport of AAIW is 12.8×10^6 m^3 s^{-1} for stations 102–106, with a reversed (eastward) flow inshore of station 106 of 4.1×10^6 m^3 s^{-1}, giving a net westward AAIW transport for stations 102–108 of 8.6×10^6 m^3 s^{-1}. This is a similar AAIW transport to the 8–12 ($\times 10^6$ m^3 s^{-1}) described in the preceding section for the 52°W section. Above $\sigma_2 = 36.0$ the rest of the North Brazil Current carries an additional net westward transport of 11.8×10^6 m^3 s^{-1} through those same stations. The North Brazil Current retroflects to leave

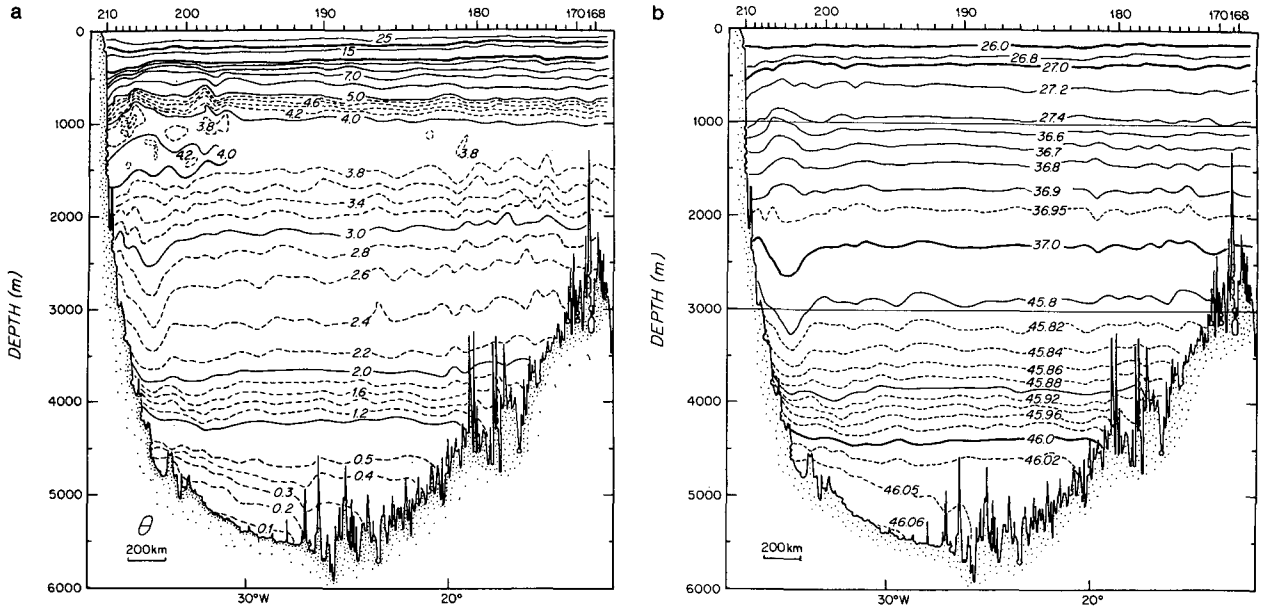

FIG. 9. Property distributions along a quasi-zonal section near 11°S made from the R/V *Oceanus* in April 1983. Station positions are shown in Fig. 1. (a) Potential temperature (°C). (b) Potential density anomaly (EOS80, kg m^{-13}). (c) Dissolved oxygen (ml l^{-1}). (d) Silicate (μmol l^{-1}). (e) Nitrate (μmol l^{-1}). (f) Salinity (psu).

the western boundary near 8°N (e.g., Johns et al. 1990).

These transport estimates of North Brazil Current components are not intended to be definitive, but only suggestive of the intensity of its flow. A definitive study would have to address more carefully the reference level issue. For the purpose of the present study, the point is that there is a sizable westward transport of low salinity and high silicate AAIW through the 37°W section above the part of the DWBC eastward flow of UNADW where the weaker northern source influence is found. There is thus a vertically superposed counterflow, and as in the case of the lateral gyre described above, there is the possibility of mixing between these opposing flows, in this case a vertical mixing.

The supposition here is that the appearance of more extreme UNADW characteristics in the offshore part of the DWBC and along the equator in the 37°W section is induced by the vertical exchange between the counterflowing southward-intensified cores of AAIW and UNADW in the inshore part of the DWBC preferentially eroding the UNADW there, rather than by an extremum of eastward advection along the equator offshore of the DWBC. In Fig. 7 the salinity, silicate, and oxygen sections are plotted with a density parameter as the vertical coordinate to illustrate better the evidence for this diapycnal property flux. The sections show departures from alignment of property isopleths with (horizontal) isopycnals occurring between the property extrema defining the AAIW and UNADW core layers. In the inner part of the DWBC, the water between the AAIW and UNADW (between σ_2 = 36.6 and 36.9) has lower salinity and higher silicate character (on isopycnals) compared to offshore which is suggestive of diapycnal diffusion between the westward flowing AAIW and the underlying eastward flowing UNADW. (Recall the ad hoc selection of σ_2 = 36.65 as the top of the NADW.) The oxygen distribution is more complex, as there is an oxygen minimum layer, the UCPW core, between the higher oxygen UNADW and the higher oxygen AAIW core. But it also fits this idea of diapycnal diffusion, from these two higher oxygen layers into the minimum layer—which is weakest (least minimum) in the south.

Such vertical exchange must be invoked to explain the downstream evolution of the AAIW in the North Brazil Current, and of the downstream erosion of the UNADW in the DWBC (contrast Figs. 4 and 6). Figure 8 illustrates this point by showing property–property plots for a station from the DWBC group along the 37°W contrasted with stations at several locations along the western boundary chosen to lie at the core of the DWBC. The southward decline of the UNADW strength (decreasing salinity and oxygen maxima, increasing silicate minimum) beneath the northward decline of the AAIW strength (increasing salinity minimum, decreasing silicate maximum and decreasing oxygen) is apparent. A deduction is that for the real ocean, as with the Kawase et al. (1992) interpretation of their model ocean, while there is eastward flow along the equator, in our case required by the isolated property extrema there, the existence of a tracer tongue

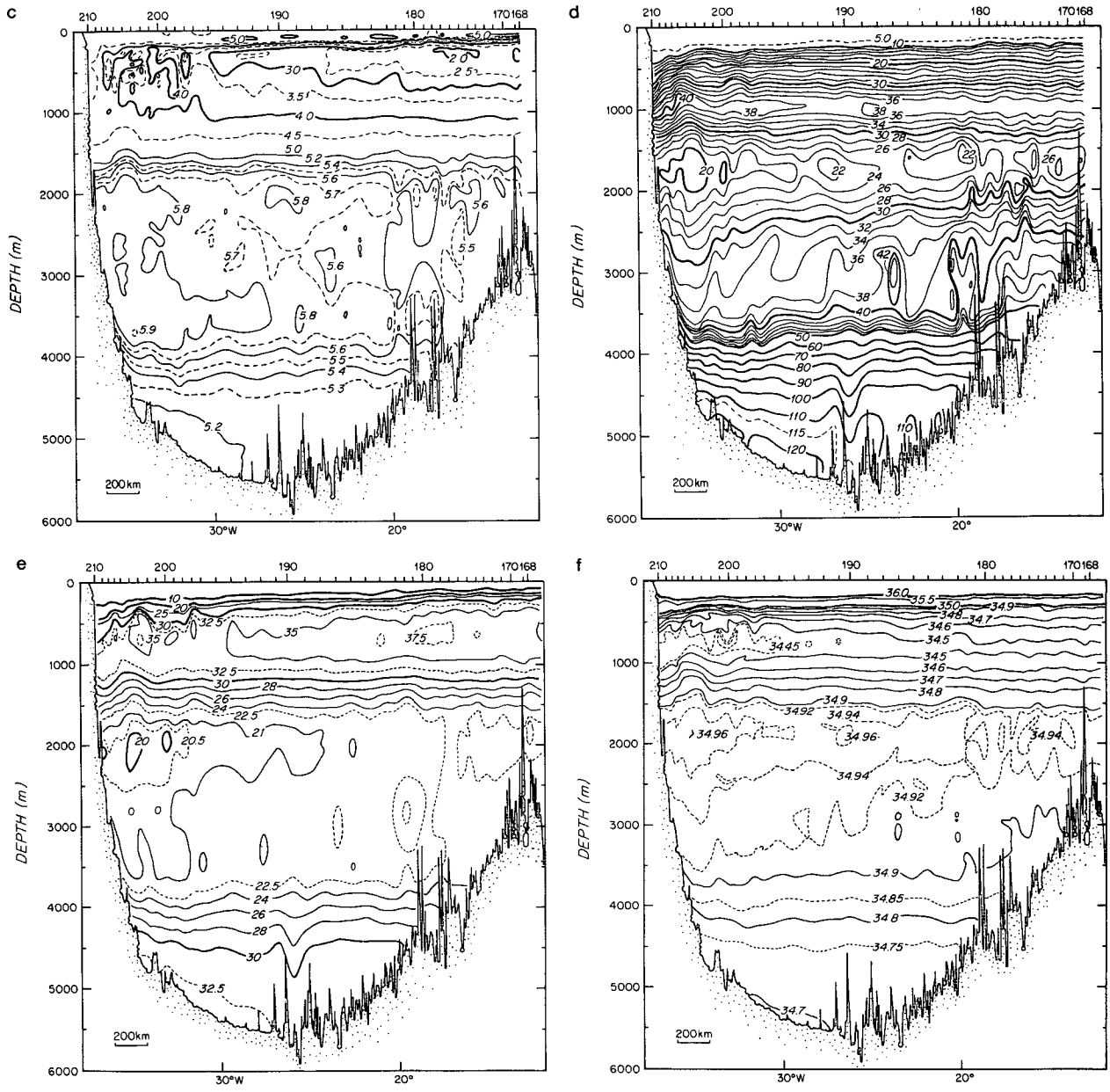

FIG. 9. (*Continued*)

isolated at the equator does not have to imply an isolation of advection there, or even that significant transport occurs there relative to that in the DWBC.

6. Gyre component to the Brazil Basin deep circulation

Moving to the midlatitudes of the Brazil Basin, Fig. 9 shows property sections from the 1983 R/V *Oceanus* section near 11°S. This section has been used to estimate AABW transport through the Brazil Basin by McCartney and Curry (1993). The shear signature of the northward flow of AABW is the broad westward rise of isotherms colder than about 1.8°C towards the western boundary. They used an LNM of 1.9°C [similar to that used by Wright (1970)], to estimate a net northward AABW transport of 5.5×10^6 m^3 s^{-1} below that isotherm. This is in general agreement with their overall scheme of AABW transport in the western Atlantic in which 4.3×10^6 m^3 s^{-1} crosses the equator in the western basin through the 37°W section (Fig. 4) with the difference between there and 11°S (1.2×10^6 m^3 s^{-1}) representing a combination of upwelling between the two locations and flow to the eastern basin

through the Romanche Fracture Zone. In the present calculations with the water masses and LNMs defined by σ_2 surfaces, a slight difference results, an AABW ($\sigma_2 \geqslant 37.1$, approximately 1.7°C at 11°S) transport of about 5.3×10^6 m^3 s^{-1} for an LNM near $\sigma_2 = 37.1$.

Figure 10a shows the dependence of NADW and AABW transports for this complete Brazil Basin transect as a function of LNM. Shallow LNM choices do not "work" for they give a net southward flow of AABW, very small southward or even northward transport of NADW, and very large northward transport of AAIW. Northward net AABW transport occurs for LNMs deeper than $\sigma_2 = 37.01$, and also net southward transport of NADW for LNMs deeper than $\sigma_2 = 37.04$. For LNMs between $\sigma_2 = 37.04$ and 37.14, all layers have net flows in the "right" directions, and the transport magnitudes depend strongly on the LNM position within this transition layer between NADW and AABW. An LNM at $\sigma_2 = 37.09$ (roughly $\theta = 1.9$°C at this latitude) gives the aforementioned AABW transport of 5.3×10^6 m^3 s^{-1}, which combined with a net southward NADW transport of 20.4×10^6 m^3 s^{-1} gives a net southward transport of cold water of 15.1, the expected magnitude of the net meridional overturning cell.

This net is achieved, however, in a curious manner: the temperature section, Fig. 9a, shows NADW isotherms below 3.5°C steeply descending eastward from the western boundary to a maximum depth, then almost equally steeply rising eastward, thus defining a gyre component to the deep flow near the western boundary. Figure 10b shows net transports through this western concentrated gyre. Only part of the net AABW transport flows through the gyre stations, but the net NADW transport through the gyre is essentially identical to the section net of Fig. 10a (for the $\sigma_2 = 37.09$ LNM, 19.1×10^6 m^3 s^{-1} compared to 20.4×10^6 m^3 s^{-1}). For the $\sigma_2 = 37.09$ LNM, the southward flowing element of this gyre (stations 203–210, Fig. 10c) transports 41.8×10^6 m^3 s^{-1} of NADW, while the northward element (stations 200–203, Fig. 10c) returns 22.7×10^6 m^3 s^{-1} flow of 4.3×10^6 m^3 s^{-1}.

Thus, the net NADW flow in the Brazil Basin is achieved through a background recirculating gyre of about equal transport amplitude, with the DWBC thus transporting southward about twice the net southward flow of NADW in the western basin. This Brazil Basin abyssal gyre is similar in intensity to the Guiana abyssal gyre, whose gyre component is more or less equal to the net flow. Both are counterclockwise gyres, but the change of sign of the Coriolis parameter makes the Brazil abyssal gyre anticyclonic and the Guiana abyssal gyre (north of the equator) cyclonic. The latter gyre includes a recirculating AABW component, the former does not. It is beyond the scope of the present study to give a complete discussion of the 11°S section and the deep circulation of the Brazil Basin. A natural question is whether the Guiana and Brazil abyssal gyres are simply connected. It seems doubtful that the DWBC completely disassembles and reassembles itself between 2° and 11°S, and thus it seems reasonable to assume that at least some part of the DWBC directly flows from the 37°W section to the 11°S section.

It is less certain, however, what the narrow recir-

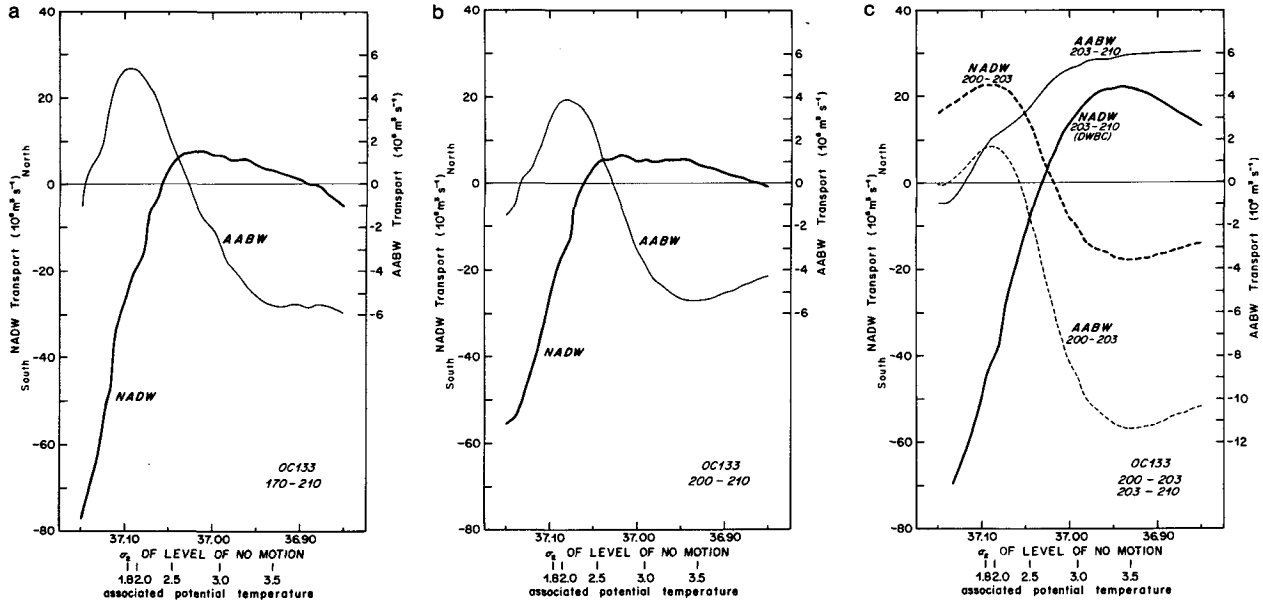

FIG. 10. Transports (10^6 m^3 s^{-1}) of AABW and NADW for parts of the 11°S section of Fig. 9. NADW defined as the layer between $\sigma_2 = 37.1$ and 36.65, and AABW as all water denser than $\sigma_2 = 37.1$. (a) Section net transport (stations 170–210). (b) Abyssal gyre net transport (stations 200–210). (c) DWBC transport (stations 203–210) and its gyre recirculation (stations 200–203).

culation at 11°S does between there and the equator. That is, where does the real ocean fall between the two extremes of complete connection or disconnection of the northward flowing limbs of the two abyssal gyres shown as Figs. 2a and 2b? The temperature distributions along the IGY sections at 8°S and 16°S show aspects of the isotherm "bowl" pattern seen at 11°S (Fig. 9a). At 16°S, Fig. 11a, the field looks like an underresolved version of the 11°S section, with the station placement catching a similar maximum depth in the isotherm bowl, but with the onshore rise of isotherms in the DWBC probably incompletely defined due to the great bottom depth difference between stations 121 and 122. Stommel et al. (1983) show a later reoccupation of the western part of this 16°S section, with much more closely spaced stations at the steep part of the western boundary, and better defining the bowl and onshore rise.

In the 8°S IGY section, Fig. 11b, a suggestion of a bowl in the deep-water isotherm is also indicated, but the station spacing is at best a marginal sampling of the DWBC regime because of the large distance between stations 116 and 117, and the steepness of the boundary between stations 118 and 119. In particular, the isotherm bowl could be deeper than drawn between stations 116 and 117. A near reoccupation of part of the IGY 8°S section occurred in the expedition collecting the CFC dataset of Fig. 3; its distribution of temperature and potential density (Scripps Institution of Oceanography 1986) is shown in Fig. 12. In the NADW the DWBC is fairly narrow, west of station 128 or 129. East of station 129 deep-water isotherms and isopycnals rise eastward over the remainder of the sections, indicating a broader recirculation than at 11°S, although there is a degree of concentration of the shear hinted at by the steep slope of the 2.8 and 2.6°C isotherms between stations 127 and 128. A 1.9°C thermostad creates an isotherm bump at station 128 to complicate the shear further, causing the bowl to disappear below about 2.3°C (3300 m) compared to its penetration to 1.8°C (3700 m) at 11°S (Fig. 9a).

The station placing on the sections between 16° and 8°S leaves some uncertainty to the structure of the Brazil Basin abyssal gyre. The lack of sections between 8°S and the 37°W section across the equator leaves unresolved for now the relationship of the Guiana and Brazil Basin abyssal gyres. There are some hints in the property distributions for the 37°W and 11°S sections of possible complexity in that relationship—although given the preceding discussions of the difficulty in interpreting the circulation paths from property tongues, caution in deducing too much from those hints is needed. There is a range of circulation "models" between the two extremes (Fig. 2) of complete connection or complete disconnection of the northward flowing limbs of the gyres—assuming that part of the DWBC flow is continuous.

At 11°S (Fig. 9) there is very little property contrast in the NADW between the two sides of the bowl, indicative of the homogenizing action of the recirculation. In the lower NADW, silicate is higher and oxygen lower than in the DWBC just south of the equator at 37°W. Charts of silicate, oxygen, and salinity on two density surfaces (near 1.9° and 2.2°C) by Speer and

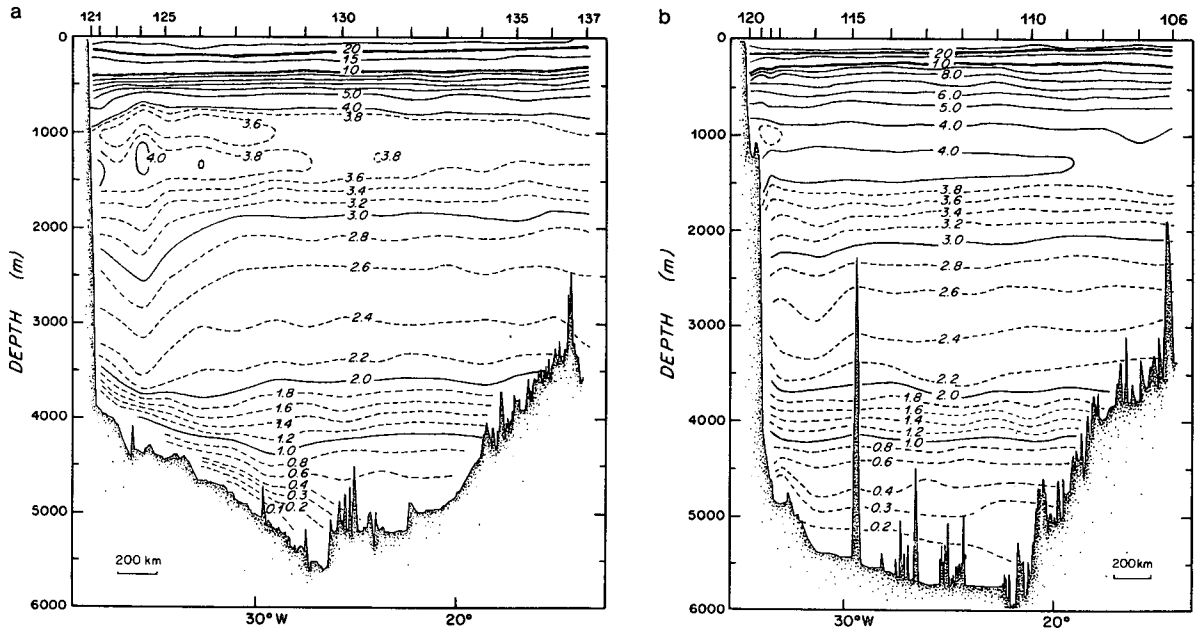

FIG. 11. Potential temperature distributions from zonal sections made from the R/V *Crawford* in March–April 1957 (Fuglister 1960). Station positions are shown on Fig. 1. (a) 16°S; (b) 8°S.

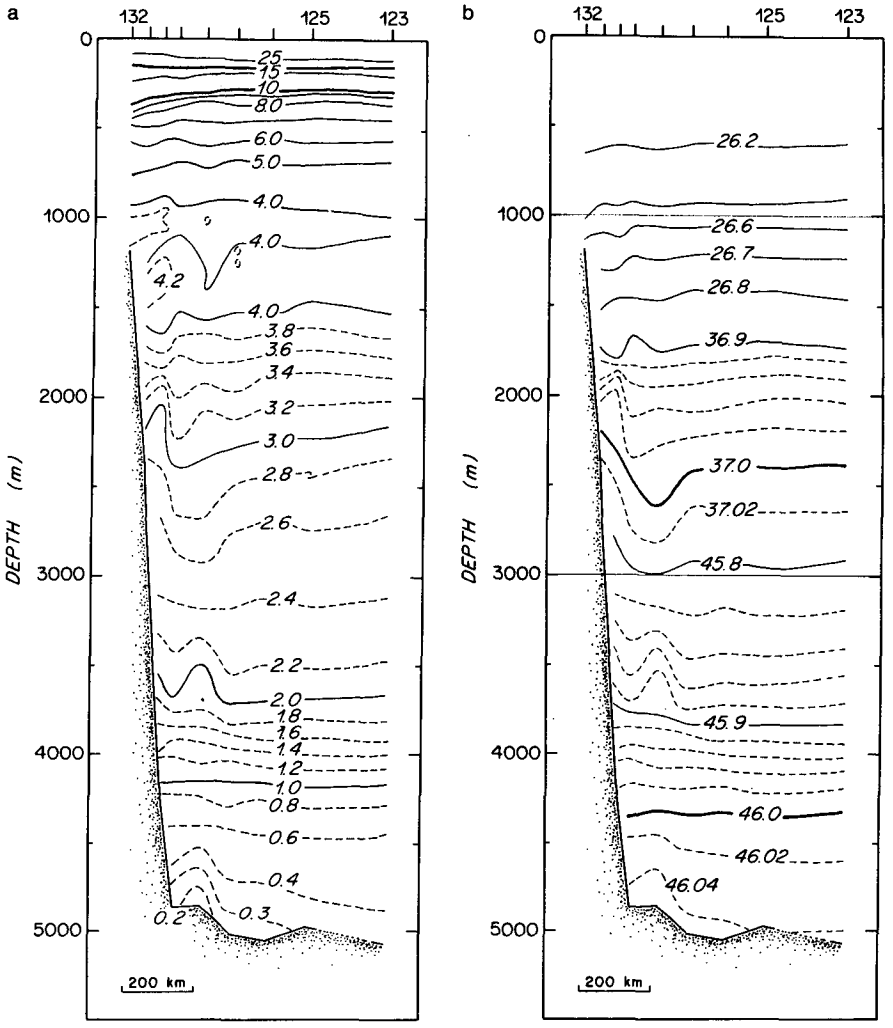

FIG. 12. Property distributions along the 8°S section segment from the data used in Fig. 3. Station positions are shown in Fig. 1. (a) Potential temperature (°C). (b) Potential density (EOS80, kg m^{-3}).

McCartney (1991) also show the steep decline in NADW characteristics along the western boundary of the Brazil Basin. These changes in the DWBC water mass presumably reflect the dilution of the northern source characteristics by the action of the recirculation, and suggest the impact of confluence of interior water into the DWBC. This is consistent with the growth in southward transport between the equator and 11°S from 35 to 42 ($\times 10^6$ m^3 s^{-1}), and also with lateral diffusive exchange between the opposing flows of the two limbs of the gyre. In Fig. 3, it is presumably this dilution that causes the weakness of the UNADW CFC concentration along the western boundary of the Brazil Basin, not a weakness of the flow. But, without data between the equator and 8°–11°S, there are two extremes of ways to achieve this dilution and confluence. The disconnected gyres extreme, sketched as Fig. 2a, has the DWBC first decline from 35×10^6 m^3 s^{-1} to some small number like the expected basin net flow of 15×10^6 m^3 s^{-1}, and then rise to the 42×10^6 m^3 s^{-1} estimated at 11°S. The connected gyres extreme, sketched as Fig. 2b, has the DWBC steadily gain transport from confluence of flow from the northward limb of the gyre.

There are elements of both these extreme interpretations hinted at by the property distributions. Evidence for the connected gyres extreme is found at 2.3°C, for the high silicate cat's eyes at 37°W (Fig. 4), which must come from the Southern Hemisphere, and the corresponding oxygen values are a good match for the characteristics in the Brazil Basin abyssal gyre at 11°S at that same temperature (Fig. 9). Immediately below this temperature at 2.1°C, however, is evidence for the disconnected gyres extreme, for the low silicate and high oxygen visible in the equatorial channel above the AABW at 37°W do not match the properties at 11°S,

suggesting that DWBC flow lines have turned back to the north between the two locations. Rather different pathways thus seem to be indicated for these slightly different levels. This demonstrates the difficulty in completing a circulation scheme near the equator, where the lack of geostrophic shear measurement forces reliance on the property fields for inference of the flow. While high vertical mode number structure cannot be ruled out at the equator given observations of deep jets at the equator (Ponte et al. 1990) and given the controversial layered jets in some numerical models (discussed in section 2), the structures suggested by the nuances of the property fields may not turn out to reflect the reality of the flow when direct current measurements become available. Whatever the flow underlying the silicate cat's eyes at 37°W is, it does seem to be a permanent circulation rather than an eddy disturbance, for the same sort of silicate distribution has been seen at this location two other times: during the 1972 GEOSECS Atlantic expedition (Bainbridge 1980, 1981) and in 1989 (Scripps Institution of Oceanography 1992; McCartney and Curry 1993), with the same degree of extrema at the same temperature as in the 1983 37°W section.

7. Summary

Property distributions, including geostrophic shear, along a section intersecting the western boundary of the Brazil Basin immediately south of the equator show that the DWBC directly crosses the equator along the western boundary. The lower and middle levels of the NADW show a concentration of northern source influence in this DWBC regime south of the equator. In the UNADW, while the shear signature of the DWBC is still established against the continental slope south of the equator, the most extreme northern source influence is displaced offshore. This appears to reflect not a shift of the dominant flow path but rather the impact of downgradient property fluxes between the AAIW and UNADW, which are superposed and flowing in opposite directions along the western boundary, strongly eroding the UNADW in the DWBC south of the equator. The DWBC at low latitudes in both hemispheres is found to transport considerably more NADW than the expected net flow, and the excess is recirculated in abyssal gyres in the Guiana and Brazil basins, with the former extending into the Southern Hemisphere, and with the degree of connectedness of the two recirculations not established. These recirculating gyres dilute the northern source influence in the DWBC with Southern Hemisphere influence, and the recirculating aspect is a "self-mixing" process that makes deduction of flow speed and water ages from tracer signals problematic. In essence, one needs a quantitative "model" of the actual circulation to interpret the tracers. The reverse, deducing the circulation from the evolving tracer fields, for example, using intruding tracer tongues, in the absence of shear measurements to constrain the range of circulations seems a nonunique determination. This recalls and confirms the cautionary recognition by Weiss et al. (1985) that their estimates of DWBC source water dilution and advection speeds "are strongly model dependent."

Acknowledgments. The author thanks Ray Weiss, Mitsuhiro Kawase, and Lew Rothstein for making available unpublished CFC and model results, and Bruce Warren for occupying and making available the fine 11°S *Oceanus* section data. Theresa Turner and Ruth Curry are thanked for their careful work in preparing the analysis products reported on here. Discussions with Rana Fine, Marjy Friedrichs, Mindy Hall, Bill Johns, Bob Molinari, and Bob Pickart helped clarify the interpretations described here, as did the remarks of the referees. This work was supported by the National Science Foundation under Grants OCE86-14486 and OCE91-05834, and the Atlantic Climate Change Program of the National Oceanic and Atmospheric Administration under Grant NA16RC0528-01.

REFERENCES

Bainbridge, A. E., 1980: *GEOSECS Atlantic Expedition.* Vol. 2, *Sections and Profiles.* National Science Foundation, 196 + xiv pp.

——, 1981: *GEOSECS Atlantic Expedition.* Vol. 1, *Hydrographic Data 1972–1973.* U.S. Govt. Printing Office, Washington, DC, 121 pp.

Bennett, S. L., and M. S. McCartney, 1990: The large transport deep western boundary current and its recirculation in the low latitude Atlantic. *Eos, Trans. Am. Geophys. Union,* **71,** 168. [Abstract.]

——, ——, and M. L. Bremer, 1983: Some aspects of the deep circulation of the tropical North Atlantic. *Eos, Trans. Am. Geophys. Union,* **64,** 1027. [Abstract.]

Bullister, J. L., and R. F. Weiss, 1983: Anthropogenic chlorofluoromethanes in the Greenland and Norwegian seas. *Science,* **221,** 265–268.

Fine, R. A., and R. L. Molinari, 1988: A continuous deep western boundary current between Abaco (26.5°N) and Barbados (13°N). *Deep-Sea Res.,* **35,** 1441–1450.

Friedrichs, M. A. M., 1992: Meridional circulation in the tropical North Atlantic. M.S. thesis, MIT and WHOI Joint Program, Woods Hole, Massachusetts, 88 pp.

Fuglister, F. C., 1960: Atlantic Ocean atlas of temperature and salinity profiles and data from International Geophysical Year of 1957–1958. Woods Hole Oceanographic Institution Atlas Series, **1,** 209 pp.

Hall, M., and H. Bryden, 1982: Direct estimates and mechanisms of ocean heat transport. *Deep-Sea Res.,* **29,** 339–359.

Hogg, N., P. Biscaye, W. Gardner, and W. J. Schmitz, Jr., 1982: On the transport and modification of Antarctic Bottom Water in the Vema Channel. *J. Mar. Res.,* **40,** 231–263.

Johns, W. E., D. M. Fratantoni, and R. J. Zantopp, 1993: Deep western boundary current variability off northeastern Brazil. *Deep-Sea Res.,* **40,** 293–310.

——, T. N. Lee, F. A. Schott, R. J. Zantopp, and R. M. Evans, 1990: The North Brazil Current retroflection: Seasonal structure and eddy variability. *J. Geophys. Res.,* **95,** 22 103–22 120.

Kawase, M., 1987: Establishment of deep ocean circulation driven by deep water production. *J. Phys. Oceanogr.,* **17,** 2294–2316.

——, L. M. Rothstein, and S. R. Springer, 1992: Encounter of the deep western boundary current with the equator: A spin-up numerical experiment. *J. Geophys. Res.,* **97**(C4), 5447–5463.

Knapp, G. P., and H. M. Stommel, 1985: Hydrographic data from R. V. *Oceanus* Cruise 133, leg VII. Woods Hole Oceanographic Institution Tech. Rep. WHOI-85-38, 107 pp.

Leaman, K. D., and J. E. Harris, 1990: On the average absolute transport to the deep western boundary currents east of Abaco Island, the Bahamas. *J. Phys. Oceanogr.*, **20,** 467–475.

Lee, T. N., W. Johns, F. Schott, and R. Zantopp, 1990: Western boundary current structure and variability east of Abaco Bahamas at 26.5°N. *J. Phys. Oceanogr.*, **20,** 446–466.

McCartney, M. S., 1990: Trans-equatorial flow of deep and bottom water in the western Atlantic Ocean. *Eos, Trans. Am. Geophys. Union,* **71,** 168. [Abstract.]

——, 1993: The transport of Antarctic Bottom Water at 4°N in the western basin of the North Atlantic Ocean. *J. Geophys. Res.*, in press.

——, and R. A. Curry, 1993: Transequatorial flow of Antarctic Bottom Water in the western Atlantic Ocean: Abyssal geostrophy at the equator. *J. Phys. Oceanogr.*, **23,** 1264–1276.

——, S. L. Bennett, and M. E. Woodgate-Jones, 1991: Eastward flow through the mid-Atlantic ridge at 11°N and its influence on the abyss of the eastern basin. *J. Phys. Oceanogr.*, **21,** 1189–1121.

Molinari, R. L., R. A. Fine, and E. Johns, 1992: The deep western boundary current in the tropical North Atlantic Ocean. *Deep-Sea Res.*, **39,** 1967–1984.

Pickart, R. S., N. G. Hogg, and W. M. Smethie, Jr., 1989: Determining the strength of the deep western boundary current using the chlorofluoromethane ratio. *J. Phys. Oceanogr.*, **19**(7), 940–951.

Ponte, R. M., J. Luyten, and P. L. Richardson, 1990: Equatorial deep jets in the Atlantic Ocean. *Deep-Sea Res.*, **37**(4), 711–713.

Reid, J., and A. W. Mantyla, 1989: Circumpolar water in North Atlantic. *Eos, Trans. Am. Geophys. Union,* **70,** 1132. [Abstract.]

Richardson, P. R., and W. J. Schmitz, Jr., 1993: Deep cross-equatorial flow in the Atlantic measured with SOFAR floats. *J. Geophys. Res.*, in press.

Schmitz, W. J., Jr., and M. S. McCartney, 1993: On the North Atlantic circulation. *Rev. Geophys.*, **31,** 29–49.

Scripps Institution of Oceanography, 1986: Shipboard physical and chemical data report: Transient Tracers in the Ocean Tropical Atlantic Study, 1 December 1982–18 February 1983. Scripps Institution of Oceanography, University of California, SIO Ref. 86-16, 300 pp.

——, 1992: Hydros Leg 4: Physical, chemical and CTD data, 13 March–19 April 1989, R/V *Melville.* Scripps Institution of Oceanography, University of California, SIO Ref. 92-12, 190 pp.

Speer, K. G., and M. S. McCartney, 1991: Tracing lower North Atlantic Deep Water across the equator. *J. Geophys. Res.*, **96,** 20 443–20 448.

Stommel, H., and A. B. Arons, 1960: On the abyssal circulation of the world ocean—I. Stationary planetary patterns on a sphere. *Deep-Sea Res.*, **6,** 140–154.

——, R. J. Stanley, G. P. Knapp, R. Knox, and A. Amos, 1983: Descent of bottom water along the rise in the Brazilian Basin. *J. Phys. Oceanogr.*, **13,** 554–558.

Suginohara, N., and M. Fukasawa, 1988: Set-up of deep circulation in multi-level numerical models. *J. Oceanogr. Soc. Japan,* **44,** 315–336.

——, and S. Aoki, 1991: Buoyancy-driven circulation as horizontal convection on a β-plane. *J. Mar. Res.*, **49,** 295–320.

——, ——, and M. Fukasawa, 1991: Comment on "On the importance of vertical resolution in certain ocean general circulation models." *J. Phys. Oceanogr.*, **21,** 1699–1701.

Weaver, A. J., and E. S. Sarachik, 1990: On the importance of vertical resolution in certain ocean general circulation models. *J. Phys. Oceanogr.*, **20,** 600–609.

——, and ——, 1991: Reply. *J. Phys. Oceanogr.*, **21,** 1702–1707.

Wallace, D. W. R., and J. R. N. Lazier, 1988: Anthropogenic chlorofluoromethanes in newly formed Labrador Sea Water. *Nature,* **332,** 61–63.

Warren, B. A., 1981: Deep water circulation in the world ocean. *Evolution of Physical Oceanography: Scientific Surveys in Honor of Henry Stommel,* B. A. Warren and C. Wunsch, Eds., The MIT Press, pp. 6–41.

Weiss, R. F., J. L. Bullister, R. H. Gammon, and M. J. Warner, 1985: Atmospheric chlorofluoromethanes in the deep equatorial Atlantic. *Nature,* **314,** 608–610.

——, M. J. Warner, K. G. Harrison, and W. M. Smethie, 1989: Deep equatorial Atlantic chlorofluorocarbon distributions. *Eos, Trans. Am. Geophys. Union,* **70,** 1132. [Abstract.]

Wright, W. R., 1970: Northward transport of Antarctic Bottom Water in the western Atlantic Ocean. *Deep-Sea Res.*, **17,** 367–371.

Wunsch, C., 1978: The North Atlantic general circulation west of 50°W determined by inverse methods. *Rev. Geophys. Space Phys.*, **16,** 583–620.

——, and B. Grant, 1982: Towards the general circulation of the North Atlantic Ocean. *Progress in Oceanography,* Vol. 11, Pergamon, 1–59.

Wüst, G., 1935: Schichtung und Zirkulation des Atlantischen Ozeans. Die Stratosphäre. *Wissenschaftliche Ergebnisse der Deutschen Atlantischen Expedition auf dem Forschungs und Vermessungsschiff "Meteor,"* 1925–1927, Vol. 6(1), 180 pp. [English translation in the *Stratosphere of the Atlantic Ocean,* W. J. Emery, Ed., 1978, Amerind, 112 pp.]